



Review

# The Value of Electroretinography in Identifying Candidate Genes for Inherited Retinal Dystrophies: A Diagnostic Guide

Tsai-Hsuan Yang<sup>1,2</sup>, Eugene Yu-Chuan Kang<sup>3,4,5</sup>, Pei-Hsuan Lin<sup>6,7</sup>, Pei-Liang Wu<sup>7,8</sup>, Jacob Aaron Sachs<sup>7,9</sup> and Nan-Kai Wang<sup>3,4,7,10,\*</sup>

- <sup>1</sup> Department of Education, Chang Gung Memorial Hospital, Linkou Medical Center, Taoyuan 33305, Taiwan; yangth@cgmh.org.tw
- <sup>2</sup> College of Medicine, National Yang Ming Chiao Tung University, Taipei 11217, Taiwan
- <sup>3</sup> Department of Ophthalmology, Chang Gung Memorial Hospital, Linkou Medical Center, Taoyuan 33305, Taiwan; yckang@cgmh.org.tw
- <sup>4</sup> College of Medicine, Chang Gung University, Taoyuan 33302, Taiwan
- <sup>5</sup> Graduate Institute of Clinical Medical Sciences, College of Medicine, Chang Gung University, Taoyuan 33302, Taiwan
- <sup>6</sup> National Taiwan University Hospital, Yunlin 640203, Taiwan; y04507@ms1.ylh.gov.tw
- <sup>7</sup> Department of Ophthalmology, Edward S. Harkness Eye Institute, Columbia University Irving Medical Center, Columbia University, New York, NY 10032, USA; b10401094@ntu.edu.tw (P.-L.W.); jas1068@miami.edu (J.A.S.)
- <sup>8</sup> Department of Medicine, National Taiwan University, Taipei 10617, Taiwan
- <sup>9</sup> College of Arts and Sciences, University of Miami, Coral Gables, FL 33146, USA
- <sup>10</sup> Vagelos College of Physicians and Surgeons, Columbia University, New York, NY 10032, USA
- \* Correspondence: nw2189@cumc.columbia.edu

**Abstract:** Inherited retinal dystrophies (IRDs) are a group of heterogeneous diseases caused by genetic mutations that specifically affect the function of the rod, cone, or bipolar cells in the retina. Electroretinography (ERG) is a diagnostic tool that measures the electrical activity of the retina in response to light stimuli, and it can help to determine the function of these cells. A normal ERG response consists of two waves, the a-wave and the b-wave, which reflect the activity of the photoreceptor cells and the bipolar and Muller cells, respectively. Despite the growing availability of next-generation sequencing (NGS) technology, identifying the precise genetic mutation causing an IRD can be challenging and costly. However, certain types of IRDs present with unique ERG features that can help guide genetic testing. By combining these ERG findings with other clinical information, such as on family history and retinal imaging, physicians can effectively narrow down the list of candidate genes to be sequenced, thereby reducing the cost of genetic testing. This review article focuses on certain types of IRDs with unique ERG features. We will discuss the pathophysiology and clinical presentation of, and ERG findings on, these disorders, emphasizing the unique role ERG plays in their diagnosis and genetic testing.

**Keywords:** electroretinography; inherited retinal dystrophies; electronegative ERG; congenital stationary night blindness; X-linked retinoschisis; cone-rod dystrophies; fundus albipunctatus; enhanced S-cone syndrome; cone dystrophy with supernormal rod response



**Citation:** Yang, T.-H.; Kang, E.Y.-C.; Lin, P.-H.; Wu, P.-L.; Sachs, J.A.; Wang, N.-K. The Value of Electroretinography in Identifying Candidate Genes for Inherited Retinal Dystrophies: A Diagnostic Guide. *Diagnostics* **2023**, *13*, 3041. <https://doi.org/10.3390/diagnostics13193041>

Academic Editor: Jae-Ho Han

Received: 20 August 2023

Revised: 8 September 2023

Accepted: 13 September 2023

Published: 25 September 2023



**Copyright:** © 2023 by the authors. Licensee MDPI, Basel, Switzerland. This article is an open access article distributed under the terms and conditions of the Creative Commons Attribution (CC BY) license (<https://creativecommons.org/licenses/by/4.0/>).

## 1. Introduction

### 1.1. Background and Significance of Electroretinography (ERG)

Inherited retinal dystrophies (IRDs) stem from genetic mutations. In addition to clinical and imaging assessments, identifying these mutations is crucial for a definitive diagnosis, which can lead to improved disease classification and pathophysiology research.

Though genome sequencing costs are decreasing rapidly [1], using multimodal ophthalmic examinations to narrow the differential diagnosis and sequence only the disease-associated genes is still preferred. Sequencing a patient's entire genome is utilized less

due to certain limitations. Firstly, false positive signals can be generated, and interpreting them can be challenging. Secondly, incidentally found genetic mutations that have no onset or have low penetrance are possible. Deciding whether or not to inform a patient of these mutations requires careful ethical consideration, well-established policies, and an evaluation of the cost-effectiveness and benefits of any further preventative measures [2,3].

Therefore, narrowing the differential diagnosis before ordering disease-specific candidate gene sequencing is crucial. To achieve this, it is necessary to look into the personal and family history of the patient and conduct multiple ophthalmic examinations that complement each other's diagnostic limitations. Diseases of the inner retina may be associated with a normal fundus appearance. While optical coherence tomography (OCT) is a valuable tool in detecting structural abnormalities in different retina layers, functional retinal dysfunction requires electrophysiological examinations for proper diagnosis. Full-field ERG (ffERG) distinguishes between generalized outer or inner retinal abnormalities and determines whether the dysfunction is predominantly in the bipolar cells or photoreceptors (rod or cone cells).

This review aims to offer guidance on using ffERG to pinpoint potential genes for sequencing, leading to a conclusive diagnosis. We cover the physiological basis of ERG to aid in understanding the origin and formation of ERG features in IRDs. Our focus is on monogenic IRDs that display distinct ERG patterns, where we discuss the pathophysiology, clinical presentation, ERG features, and genes responsible for these diseases.

### 1.2. Anatomy and Physiology of the Retina

The vertebrate retina consists of ten anatomical layers. The retinal pigmented epithelial cells (RPE) provide support for the neural retina, which is mainly composed of three types of neurons connected in the following order: photoreceptors, bipolar cells, and ganglion cells.

The retina's photoreceptor layer comprises rods and cones with different visual functions, distributions, and connections to post-synaptic bipolar cells. The outer segments of photoreceptors contain photopigments consisting of chromophore 11-*cis*-retinal and opsins. Rhodopsins are the photopigments in rods that provide monochromatic vision. Rods are sensitive to single photons, making them important for visual perception in dim light. Conversely, cones function in well-lit conditions and are responsible for color perception through short, middle, and long opsins. Rods are more densely packed than cones throughout most of the retina, except in the fovea, where cones are most abundant and contribute to high visual acuity in that area [4]. Rods connect to On-bipolar cells, while cones synapse to On- or Off-bipolar cells. Acknowledging the different functions, distributions, and connections to post-synaptic bipolar cells of rods and cones can aid in comprehending the various symptoms of rod- or cone-dominant IRDs and help in understanding the formation of ERG. Figure 1 displays the retina anatomy and various electrophysiological tests that gather collective cellular reactions from multiple levels of the retina. Further elaboration on these topics will be provided below.

The visual pathway is such that light stimulation on the retina leads to visual perception in the brain. This process begins with phototransduction, where light stimulates photoreceptors. The next stage, a post-receptoral process within the retina, involves bipolar and ganglion cell activation. Finally, the signal transmits beyond the retina, through the lateral geniculate nucleus, and to the brain's visual cortex, forming a visual perception. The initial two stages of the visual process, which occur in the retina, will be covered here.

The process of phototransduction in photoreceptors converts photons into electrophysiological signals by bleaching photopigments, which requires the visual cycle between photoreceptors and RPE cells to replenish the photopigments [5]. Phototransduction begins when light stimulates 11-*cis*-retinal to isomerize into all-*trans*-retinal. This triggers conformational changes in opsins, interrupting cyclic guanosine monophosphate (cGMP) accumulation and leading to the closure of the constantly open cation channels. This, in turn, causes the photoreceptors to become hyperpolarized, decreasing the levels of glutamate released from the photoreceptors to the post-synaptic bipolar cells. To maintain

phototransduction processing, the visual cycle recycles retinoids between the photoreceptors and RPE to replenish the 11-cis-retinal in the rhodopsin. Figure 2 depicts the genes and encoded proteins involved in phototransduction and the visual cycle. Mutations in these genes can cause IRDs such as fundus albipunctatus, Oguchi retinopathy, Riggs-type CSNB, or *GUCY2D*-related cone-rod dystrophy.

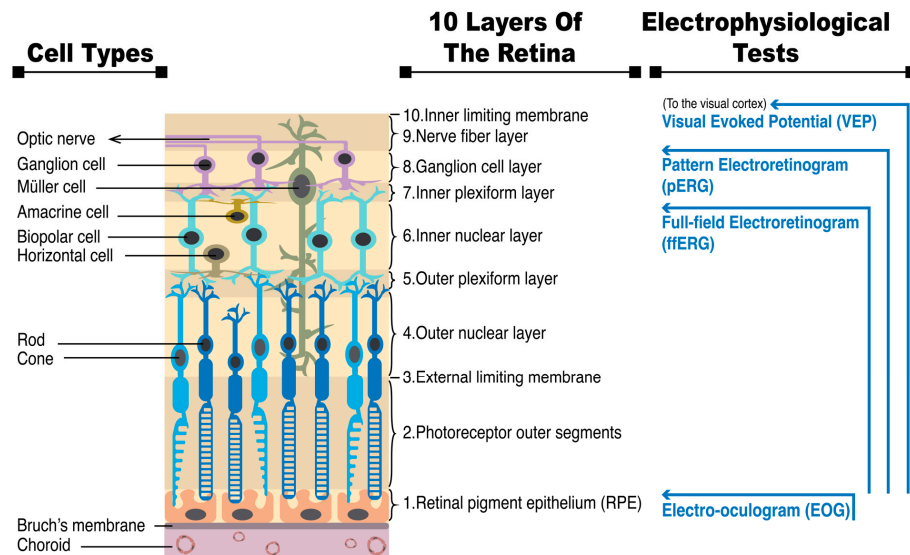


**Figure 1.** The retina anatomy and various electrophysiological tests gathering collective cellular reactions from multiple levels of the retina.

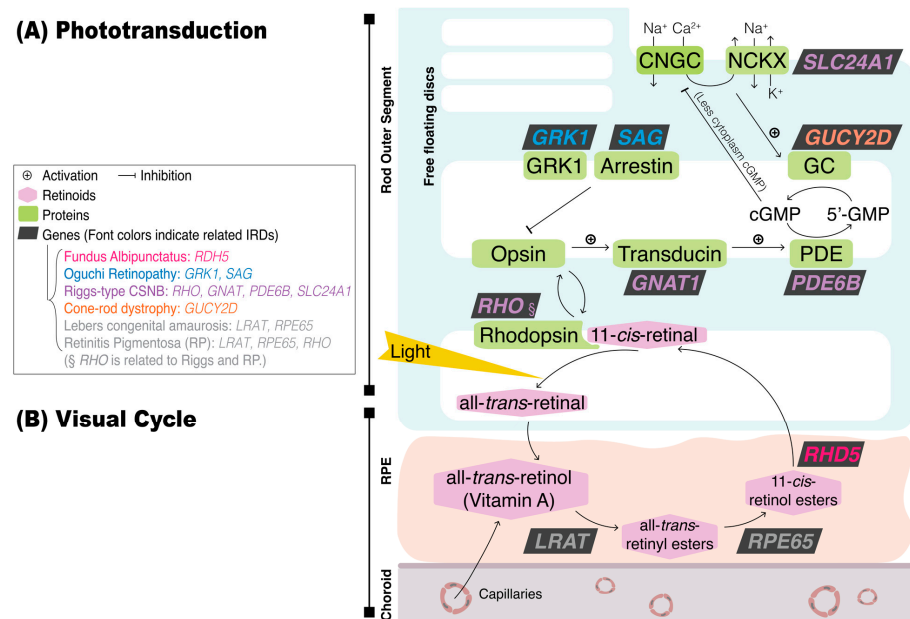


**Figure 2.** The schematic of genes and encoded proteins involved in phototransduction and the visual cycle. Genes in different colored fonts indicate the responsibility for various inherited retinal diseases (IRDs): orange for fundus albipunctatus, blue for Oguchi retinopathy, green for Riggs-type congenital stationary night blindness (CSNB), purple for *GUCY2D*-related cone-rod dystrophy, and grey for Leber congenital amaurosis or retinitis pigmentosa (RP). Genes in the graph are specifically expressed in rods, except for *GUCY2D*, expressed in both rods and cones. The diagram shows the process in rods, but the proteins used in cones are the same, except that rhodopsin should be replaced with cone-opsins. (A) *Phototransduction*. Rhodopsin is located in the outer segments of rods and consists of 11-cis-retinal chromophore and opsin. To begin, light stimulates 11-cis-retinal to isomerize into all-trans-retinal and changes the shape of opsins, activating transducin, the G-protein coupled to

rhodopsin. This, in turn, activates photoreceptor phosphodiesterase (PDE), which hydrolyzes cyclic guanosine monophosphate (cGMP) and leads to the closure of the cyclic nucleotide-gated ion channel (CNGC). Therefore, photoreceptors are hyperpolarized, reducing glutamate release to bipolar cells. The recovery of phototransduction involves two parts: first, rhodopsin activity is terminated by rhodopsin kinase (GRK1) and arrestin; second, calcium efflux through sodium/calcium-potassium exchanger (NCKX) activates guanylyl cyclase (GC), which replenishes cGMP. **(B) Visual cycle.** To maintain phototransduction processing, the visual cycle recycles retinoids between the photoreceptors and RPE to replenish 11-cis-retinal in the rhodopsin. Key enzymes involved in this process include lecithin retinol acyl transferase (LRAT), RPE65 protein, and 11-cis-retinol dehydrogenase (RDH), which are encoded by genes responsible for IRDs—*LRAT*, *RPE65*, and *RDH5*, respectively. The process requires all-trans-retinol, or vitamin A, to be repleted from choroid capillaries.

A post-receptor process in the visual pathway occurs following phototransduction in the photoreceptors. When the photoreceptors decrease glutamate release upon exposure to light, On-bipolar cells (which respond to the onset of light) depolarize, while Off-bipolar cells (which respond to the offset of light) hyperpolarize. As a result, post-synaptic ganglion cells generate action potentials projecting beyond the retina through the lateral geniculate nucleus and ultimately reach the visual cortex in the brain [6].

In the following section, we will explore how ERG can aid in identifying issues in phototransduction or post-receptor processes within the retina.

### 1.3. Principles of ERG Recording and Methodological Details

Electrophysiological examinations are essential in diagnosing the functional integrity of the visual system. As displayed in Figure 1, various tests assess different parts of the visual system, such as the visual evoked potentials (VEPs) for the whole visual pathway from the eye to the visual cortex of the brain, electro-oculogram (EOG) for the outer retina and RPE, pattern ERG (pERG) to differentiate between the functions of macular and retinal ganglion cells, and multifocal ERG (mfERG) for testing multiple discrete areas of the retina simultaneously [7–10]. This article specifically focuses on the use of ffERG in diagnosing IRDs. This test measures the massed electrical response of the retina to light stimuli, allowing for the assessment of generalized retinal function involving the rod, cone, and bipolar cells.

To ensure consistency in recording ERG tests, the International Society for Clinical Electrophysiology of Vision (ISCEV) has established standards [11]. This facilitates cross-laboratory comparisons and is crucial for research on retinal diseases and accurate patient monitoring over time. Electrodes are attached to the cornea, bulbar conjunctiva, or skin of the lower eyelids of an electrically isolated patient according to the ISCEV standard protocol to measure the retina's response to flashes from a Ganzfeld stimulator, which evenly illuminate the entire retina. The protocol can begin with either dark-adapted (DA), also referred to as scotopic, ERG or light-adapted (LA), also called photopic, ERG. After 20 min of dark adaptation, the retina's response to flashes of varying strengths ( $0.01$ ,  $3$ , and  $10 \text{ cd}\cdot\text{s}\cdot\text{m}^{-2}$ ) can be evaluated to assess rod-dominated retinal function (DA 0.01 ERG; DA 3 ERG; DA 10 ERG). Alternatively, a 10 min period of light adaptation can reduce rod involvement and increase the cone system's selective contributions, allowing for the recording of the retina's response to single flashes (LA 3 ERG) or high-frequency flashes (LA 30 Hz ERG) of  $3 \text{ cd}\cdot\text{s}\cdot\text{m}^{-2}$  illuminance that are superimposed on a light-adapting background. The flash durations should be at least 5 milliseconds each, and the inter-stimulus interval should be at least 2 s for DA 0.01 ERG, 10 s for DA 3 ERG, 20 s for DA 10 ERG, and 0.5 s for LA 3 ERG, allowing all components of ERG waveforms to be recorded. At least 20 ms of baseline waveform before stimuli should be included for artifact calibration.

To assist with diagnosing certain disorders, standard ERG recordings may be supplemented with additional recordings. For instance, On–Off ERG uses extended photopic

stimulation to separate the On-bipolar response to light onset and the Off-bipolar response to light offset while S-cone ERG measures the specific response of S-cones using short wavelength flashes superimposed on a background that adapts the rods and L/M-cones [12,13].

#### 1.4. ERG Waveforms and Components

In order to localize the dysfunctional site of the retina, it is essential to know the origin of the ERG components. As previously discussed, light stimulation hyperpolarizes photoreceptors, leading the bipolar cells to depolarize. This process can be recorded in the ERG waveform, where a negative “a-wave” originates from photoreceptor hyperpolarization and a positive “b-wave” signifies bipolar cell depolarization, but only if the photoreceptors are functional.

Figure 3 shows the reference ranges of the ISCEV’s standard ffERG protocols [7]. In a scotopic setting, a dim flash, not bright enough for DA 0.01 ERG to record the response from rods but bright enough to record the amplified response from the bipolar cells, generates a b-wave reflecting the rod system sensitivity [8]. Stronger flashes produce a mixed rod–cone response that is dominated by the rod system, eliciting DA 3 ERG and DA 10 ERG. Additionally, oscillatory potentials observed in the rising limb of b-waves may indicate activity in amacrine cells and retinal ganglion cells. In patients with opaque media, small pupils, or immature retinæ, DA 10 ERG may be a valuable clinical tool.

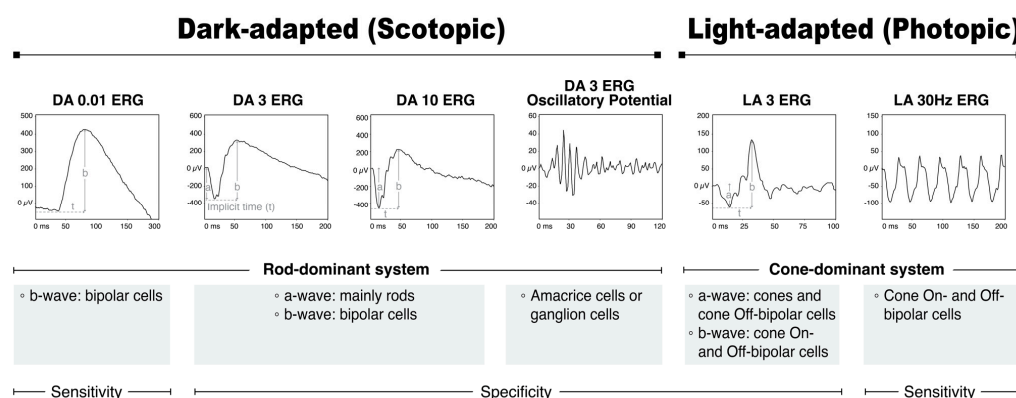


**Figure 3.** The reference ranges of standard full-field ERG (ffERG) according to the ISCEV protocol. The diagram illustrates the measurement of the amplitudes (solid vertical lines) and implicit times (broken horizontal lines marked as “t”) of the standard ERG components, which consist of a-waves and b-waves of dark-adapted (DA) and light-adapted (LA) single-flash responses. Moreover, the origins of the a-waves and b-waves in retinal cells are shown.

Alternatively, in a photopic setting where the response of the rods is saturated, LA 3 ERG and LA 30 Hz ERG reflect the cone system function. LA 3 ERG consists of an a-wave from cones and cone Off-bipolar cells and a b-wave from both the On- and Off-bipolar cells. In addition, LA 30 Hz ERG is generated by the On- and Off-bipolar cells.

Regional retinal dysfunction results in a decreased amplitude in the a- or b-wave. This is measured by looking at the baseline-to-trough region for a-waves and the trough-to-peak region for b-waves. On the other hand, a more widespread dysfunction of the retina may cause delayed “implicit time”, or the time between the light stimuli and the b-wave peak.

#### 1.5. Electronegative ERG: Pathophysiology and Associated Diseases

An electronegative waveform, also known as a waveform from negative ERG, is characterized by a smaller b-wave than the normal-sized a-wave [9]. This differs from healthy individuals, where the b-wave is larger than the a-wave. This pattern can be observed in DA 3 ERG, DA 10 ERG, or LA 3 ERG, and it pinpoints the location of retinal dysfunction as being post-receptoral, including bipolar cells or the synapse between photoreceptor and bipolar cells. Identifying this pattern can help narrow down the genes likely associated with these IRDs.



It is important to note that electronegative ERG patterns are not exclusive to IRDs [10]. They may also manifest in acquired conditions that impact one or both eyes, including but not limited to siderosis, drug toxicity, central retinal artery occlusion (CRAO), central retinal vein occlusion (CRVO), paraneoplastic or autoimmune retinopathies, and vitamin A deficiency [11–13]. It is helpful to gather information about a disease's onset time, progression course, and family history to better understand and differentiate between inherited and acquired diseases.

Here, we delve into three distinct categories that classically manifest electronegative ERG: congenital stationary night blindness (CSNB), X-linked retinoschisis (XLRN), and cone dystrophy due to *CRX* gene mutation. ERG plays a crucial role in the differential diagnosis of these conditions in order to test genes for mutations.

## 2. Congenital Stationary Night Blindness (CSNB): Riggs, Complete (cCSNB), and Incomplete (iCSNB)

### 2.1. Pathophysiology

There are four types of CSNBs, namely Riggs, Schubert–Bornschein, fundus albipunctatus, and Oguchi disease [14]. The Schubert–Bornschein type can be further categorized into complete (cCSNB) and incomplete (iCSNB) forms. This section will cover Riggs-type CSNB, cCSNB, and iCSNB, as they display distinctive ERG patterns, while the topic of fundus albipunctatus will be addressed in a separate section.

Various types of CSNB originate from genetic mutations of the different retinal cells. Riggs-type CSNB occurs due to genetic mutations that encode proteins involving rod phototransduction, leading to abnormal rods. Meanwhile, iCSNB and cCSNB are both caused by dysfunctional bipolar cells. However, iCSNB affects both On- and Off-bipolar cells due to abnormal synapses between photoreceptors and bipolar cells, while in cCSNB, the patient selectively loses the response of On-bipolar cells. Specifically, as the locus of *CACNA1F* is within the photoreceptor pre-synaptic membrane involving the release of glutamate, gene mutations of iCSNB cause both ON and OFF pathways to be affected [15]. The genetic mutations that cause cCSNB include *GRM6*, which produces glutamate receptors on the On-bipolar cells, and *TPRM1*, which generates ion channels that depolarize On-bipolar cells. Additionally, there are proteins that interact with *TPRM1* channels, including nyctalopin encoded by *NYX* and proteins expressed by *LRIT3* [16–20].

### 2.2. Clinical Presentation

Patients with CSNB commonly experience night blindness, which may be accompanied by myopia, strabismus, or nystagmus. Night blindness, or nyctalopia, typically begins before adulthood and does not progress over time, although some cases have been reported where symptoms do progress or nyctalopia is absent [21]. The presence of strabismus and nystagmus suggests that there has been a sub-optimal visual perception in the brain since the development of the visual cortex during infancy [22,23]. Patients with autosomal recessive cCSNB and *NYX* mutation often have high myopia, while those with autosomal recessive iCSNB and *CACNA1F* mutation may develop myopia or hyperopia. On the other hand, those with autosomal dominant Riggs and *RHO* mutation do not typically have myopia, strabismus, or amblyopia [24,25].

Family history, fundus imaging, and ERG are necessary tools to distinguish the different types of CSNB, which further indicate the genes to test for confirmative diagnosis. First, the types of CSNBs can be distinguished based on inheritance patterns: autosomal dominant (AD), autosomal recessive (AR), or X-linked recessive. Second, the fundus imaging of fundus albipunctatus shows small white dots scattered across the posterior pole, except on the fovea, while Oguchi disease displays a gray-white metallic sheen that disappears after dark adaptation, known as the Mizuo–Nakamura phenomenon. These fundus appearances are unique and distinguishable from Riggs-type CSNB, cCSNB, and iCSNB, which have normal fundus appearances. Lastly, their ERG patterns can differentiate cCSNB, iCSNB, and Riggs. Table 1 categorizes the types of CSNB according to fundus

appearance, inheritance pattern, and dysfunctional retinal cells and lists the reported gene mutations.

**Table 1.** Classification of congenital stationary night blindness (CSNB) and its reported gene mutations by dysfunction site, fundus appearance, and inheritance pattern.

Congenital Stationary Night Blindness (Mutated Genes)					
Dysfunctional retinal cells	Bipolar cells	iCSBN (CACNA1F) cCSNB (NYX)	N/A	iCSBN (CABP4, CACNA2D4) cCSNB (GPR170, GRM6, LRIT3, TRPM1)	N/A
	Rods	N/A	Riggs (GNAT1, PDE6B, RHO)	Riggs (SLC24A1)	Oguchi (SAG, GRK1)
	RPE	N/A	N/A	N/A	Fundus albipunctatus (RDH5)
Fundus appearance				Normal fundus	Abnormal fundus
Inheritance pattern		X-linked recessive	Autosomal dominant	Autosomal recessive	

Abbreviations: RPE, retinal pigment epithelium; iCSNB, incomplete congenital stationary night blindness; cCSNB, complete congenital stationary night blindness; N/A, not applicable.

### 2.3. ERG Findings and Candidate Genes

ERG is crucial in distinguishing the three types of CSNB with normal fundus appearance: Riggs-type CSNB, cCSNB, and iCSNB. To start, Riggs-type CSNB is identified by a flat scotopic a-wave. Next, to differentiate between cCSNB and iCSNB, which both typically display electronegative ERG reports although these are not necessary for diagnosis, photopic ERG is used.

Riggs-type CSNB has defective rods and normal cones, resulting in a flat wave in DA 3 ERG and normal photopic responses. On the other hand, iCSNB and cCSNB have post-receptoral bipolar cells that are affected but also have intact photoreceptors, causing electronegative DA ERG reports and abnormal photopic responses [26].

Photopic ERG can help distinguish between iCSNB and cCSNB. First, iCSNB has a more reduced b-wave in LA 3 ERG, consistent with abnormal synapses between cones and both On- and Off-bipolar cells. The 30 Hz flicker amplitude is severely subnormal and may display notched, or bifid, peaks [9]. Second, an LA ERG report of cCSNB has a preserved b-wave, in line with preserved Off-bipolar function. The a- and b-waves have unique shapes: the b-wave has a sharp rise and is without oscillatory potentials while the a-wave is normal with a wide trough.

If additional On–Off ERG tests are performed, the findings would be consistent with the pathophysiology: iCSNB would exhibit reduced rapid On and Off responses, while cCSNB would display a reduced rapid On response but intact rapid Off response.

The ERG findings for Riggs-type CSNB, iCSNB, and cCSNB are summarized in Table 2. Figure 4 displays a Taiwanese cohort’s fundus and ERG findings for Riggs-type CSNB, cCSNB, and iCSNB. The patients in the figure present with similar clinical features and imaging, while the distinctive ERG patterns play a pivotal role in identifying candidate genes for definitive diagnosis.

### 2.4. Differential Diagnosis, Treatments, and Prognosis

Combining Table 1 with Table 2, which outlines the ERG characteristics for these diseases, can assist in diagnosing a patient who displays symptoms of congenital stationary night blindness.

The ERG patterns of CSNBs can be indistinguishable from those of certain acquired retinal diseases. For example, the ERG pattern of cCSNB is similar to that of melanoma-associated retinopathy (MAR) due to the presence of autoantibodies against TRPM1 [27]. This is also a gene mutation responsible for cCSNB. Another example is that the ERG patterns of fundus albipunctatus and retinopathy are associated with vitamin A deficiency, which is comparable. Both conditions result from dysfunction in the retinoid cycle. Proper diagnosis requires a thorough investigation of the patient’s family and personal history,

including the onset of visual symptoms, diet, pregnancy, and any history or symptoms of cancer.

*RHO* mutations can lead to not only Riggs-type CSNB but also retinitis pigmentosa (RP). Despite both diseases being inherited in an AD pattern and presenting nyctalopia, they differ in clinical course and ERG results. *RHO*-related CSNB typically does not progress in symptoms, whereas *RHO*-related RP does. In cases of *RHO*-related CSNB, the DA 0.01 ERG report shows a flat a-wave, while the DA 3 or DA 10 ERG reports show reduced a-waves and negative b-waves. However, photopic responses remain intact, indicating that only the rods are affected. Conversely, in typical cases of *RHO*-related RP, scotopic and photopic responses are extinguished [21,28].

Several cases of CSNB are reported to be progressive, emphasizing the need for therapeutic efforts in CSNB [29,30]. Animal trials show structural recovery in *NYX*, *LRIT*, and *GRM6* knockout by adeno-associated virus (AAV)-mediated gene therapy [20,31–34]. However, unlike the success in treating *RPE65* mutations in Leber Congenital Amaurosis [35], there have not been successful human clinical trials for treating CSNB. This may be due to the fact that amblyopia and nystagmus, common symptoms of CSNB, develop during the development of the infant’s visual cortex. Therefore, it is most efficient to reverse these symptoms during the early childhood stage [36]. To accurately evaluate the benefits of clinical trials targeting amblyopia or nystagmus, younger patients within the optimal therapeutic window should be considered.

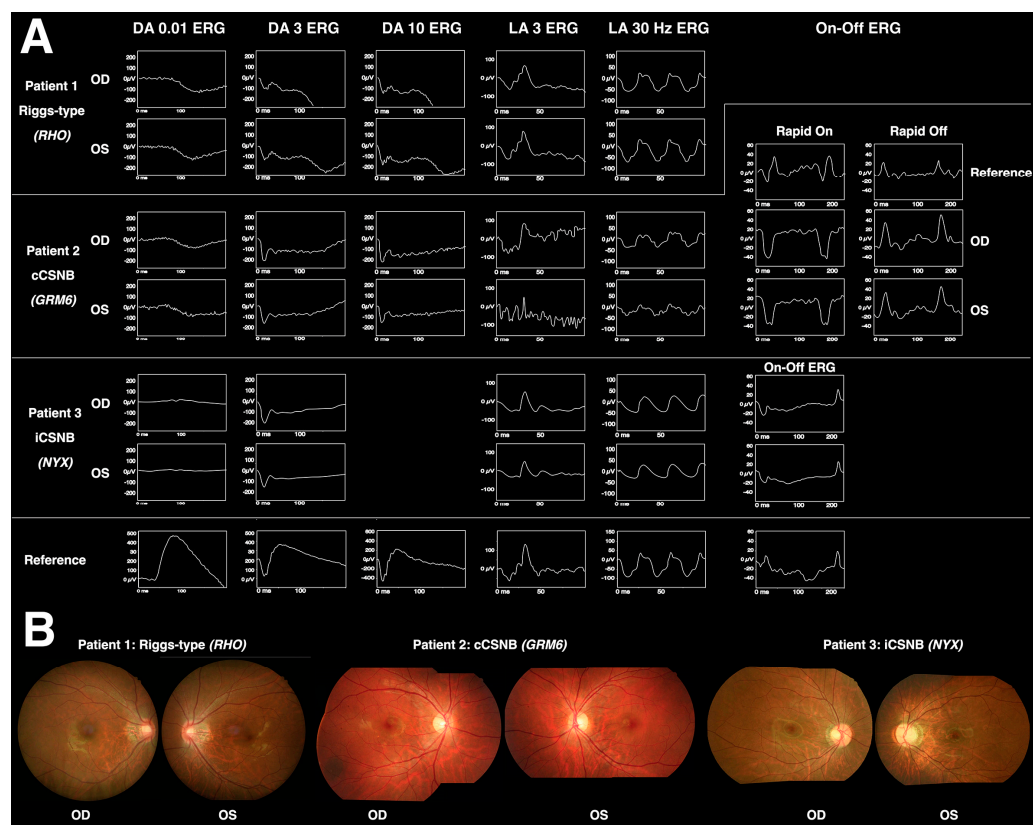


**Figure 4.** The fundus and ERG images of Riggs-type CSNB, cCSNB, and iCSNB in a Taiwanese cohort. Patient 1 has *RHO*-mutated Riggs-type CSNB, patient 2 has *GRM6*-mutated cCSNB, and patient 3 has *NYX*-mutated iCSNB. Panel (A) shows the ERG patterns, while panel (B) shows the fundus examination results. These patients present with similar clinical features and imaging, while the distinctive ERG patterns play a pivotal role in identifying candidate genes for definitive diagnosis [21].



**Table 2.** Summary of inherited retinal dystrophies with distinct electroretinography (ERG) features.

Disease	Ocular/Fundus Abnormalities	Inheritance Patterns: Mutated Genes	Scotopic ERG		Photopic ERG		Comments
			DA 0.01 ERG	DA 3 or 10 ERG	LA 3 ERG	LA 30 Hz	
<b>1. Characteristically Presents with Electronegative DA ERG</b>							
<b>Incomplete Congenital Stationary Night Blindness (iCSNB)</b>	- Sx: non-progressive nyctalopia, strabismus, nystagmus - Normal fundus - CACNA1F mutation may present myopia or hyperopia	- XR: CACNA1F - AR: CABP4, CACNA2D4	↓ ("Incompletely" abolished)	↓ b-wave (-Ve, but not required)	↓ b-wave	- ↓ amplitude & ↑ implicit time - Bifid peaks	- Affects On- and Off-bipolar cells (∴ -Ve) (∴ LA ERG more affected than cCSNB) - On-Off ERG: both ↓
<b>Complete Congenital Stationary Night Blindness (cCSNB)</b>	- Sx: same as iCSNB - NYX mutations associated with high myopia - Normal fundus	- XR: NYX - AR: GPR17, GRM6, LRIT3, TRPM1	↓↓ Extinguished ("Completely" abolished)	↓ b-wave (-Ve, but not required)	- Normal a-wave with wide trough - Preserved b-wave (sharp rise without oscillatory potentials)	Normal, possible ↑ implicit time	- Affects On-bipolar cells (∴ -Ve) (∴ Preserved b-wave in LA 3 ERG) - On-Off ERG: On↓, Off preserved - DDx: MAR (∴ anti-TRPM1)
<b>Riggs-type CSNB</b>	- Sx: RHO mutations develop nyctalopia, but not myopia, strabismus, or nystagmus - Normal fundus	- AD: GNAT, PDE6B, RHO - AR: SLC24A1	↓↓ Extinguished	↓ a-wave & ↓ b-wave (Possibly -Ve)	Normal		- Affects rods (∴ ↓ a-wave) - DDx: RHO mutation also causes <b>retinitis pigmentosa</b> (symptoms progress; both scotopic and photopic extinguished)
<b>X-linked Retinoschisis (XLRs)</b>	- Fundus: spoke-wheel appearance at the macula; could be obscured by vitreous hemorrhage - OCT: central schisis/CME, with or without peripheral schisis - FA: non-FA leakage CME	XR: RS1	↓	↓ b-wave (-Ve, but not required)	↓	↓	- Affects the synapse between photoreceptors and bipolar cells (∴ structural schisis at the neural retina) - Rx: carbonic anhydrase inhibitor (improves schisis structure but not BCVA)
<b>Cone-rod Dystrophy</b>	- Sx: ↓ visual acuity, central vision, color discrimination - Fundus: maculopathy	AD: CRX, GUCY2D, PRPH2, RAX2	↓	↓ b-wave (-Ve)	↓↓		- Cones more affected than rods - Adult onset - Progressive symptoms

Table 2. Cont.

Disease	Ocular/Fundus Abnormalities	Inheritance Patterns: Mutated Genes	Scotopic ERG		Photopic ERG		Comments
			DA 0.01 ERG	DA 3 or 10 ERG	LA 3 ERG	LA 30 Hz	
<b>2. Not characteristic of electronegative DA ERG</b>							
<b>Fundus Albipunctatus</b>	- Sx: Non-progressive nyctalopia improving after prolonged dark adaptation - Fundus: <u>White dots</u> at the posterior pole, sparing the fovea - FAF: hypo-AF signals	AR: <i>RDH5</i>	- Recovery of scotopic ERG after prolonged dark adaptation - ↓ a-wave & ↓ b-wave (Possibly -Ve)		Varies		- Affects RPE/visual cycle (∴ recovery of scotopic ERG after prolonged dark adaptation) - DDx: <b>retinitis punctata albescens</b> ( <i>RLBP1</i> gene), <b>benign retinal flecks</b>
<b>Enhanced S-cone Syndrome (ESCS)/ Goldmann-Favre Syndrome</b>	- Fundus: <u>white dots</u> at young age, round pigment clumps at the mid-periphery - OCT: CME, <u>retinal rosettes</u> - FA: non-FA leakage CME - FAF: hypo-AF signals of microglia	AR: <i>NR2E3</i>	↓↓Extinguished (∴ cone-dominated retina)	- <u>Similar waveforms in DA 3 or 10 ERG and LA 3 ERG</u> (∴ cone-dominated retina) - <u>↑LA 3 ERG a-wave</u> (∴ increased cones), which is larger than LA 30 Hz ERG wave			- ↓ cone function - ↓ rod function (∴ cone-dominated retina) - Triad of distinct ERG features - S-cone ERG: ↑ - DDx: <b>retinitis pigmentosa</b> (bone-spicule pigments at the equator)
<b>Cone Dystrophy with Supernormal Rod Response (CDSRR)</b>	- Sx: impaired central and color vision, photophobia, nyctalopia - Fundus: maculopathy - FAF: ↓ foveal, ↑parafoveal ring	AR: <i>KCNV2</i>	↓ and delayed	<u>↑ b-wave disproportionately</u>	(Cones more affected than rods)		- ↓↓ cone function and ↓ rod function - DDx: <b>hydroxychloroquine retinopathy</b> (CDSRR should not be excluded in patients taking hydroxychloroquine)

Distinct features for diagnosis are in an underlined font. Abbreviations: DA, dark-adapted; LA, light-adapted; XR, X-linked recessive; AD, autosomal dominant; AR, autosomal recessive; ↓, decreased; ↓↓, decreased more; ↑, increased; -Ve, electronegative ERG; Sx, symptoms; DDx, differential diagnosis; Rx, treatments; BCVA, best corrected visual acuity; MAR, melanoma-associated retinopathy; XLRs, X-linked retinoschisis; FA, fluorescein angiography; AF, auto-fluorescence; OCT, optical coherence tomography; FAF, fundus autofluorescence; CME, cystic macular edema; N/A, not applicable; ∴, because; ∴, therefore.

### 3. X-Linked Retinoschisis (XLRs)

#### 3.1. Pathophysiology

The cause of XLRs is a mutation in the *RS1* gene that produces the retinoschisin protein responsible for the adhesion and interaction between photoreceptors and bipolar cells [37]. When this protein is dysfunctional, it results in schisis in the neural retina.

#### 3.2. Clinical Presentation

XLRs patients experience early-onset visual loss. The fundus imaging shows cystic changes in the macula, or the typical spoke-wheel-like pattern, with or without peripheral schisis. OCT can detect cystoid macular edema (CME) in the neural retina [38,39]. Nowadays, although fluorescein angiography (FA) is not required to diagnose XLRs, it confirms the CME to be non-leaking, which can also be observed in other conditions such as nicotinic acid toxicity, enhanced S-cone syndrome, and optic pit-related macular edema [40].

There is a wide range of phenotypes in XLRs patients, which may differ significantly among or within families with the same variants. In younger patients, the spoke-wheel pattern in the fundus imaging may be obscured by conditions such as vitreous hemorrhage, retinal detachment, and leukocoria mimicking Coat-like disease [40–43]. It is important for clinicians to consider the possibility of XLRs in young patients who present with unsatisfactory BCVA along with vitreous hemorrhage or leukocoria. In older patients, macula schisis may resolve, leaving atrophic changes.

#### 3.3. ERG Findings and Diagnostic Criteria

XLRs patients have dysfunctional synapses between photoreceptors and bipolar cells, resulting in both the typical electronegative findings in DA 3 ERG as well as reduced scotopic response. However, it is important to note that not all patients with XLRs will have an electronegative scotopic ERG report, and a normal b/a ratio in their DA test results does not necessarily rule out the diagnosis of XLRs [40]. Figure 5 displays typical fundus, FA, OCT, and ERG findings in a Taiwanese cohort of XLRs patients [40].

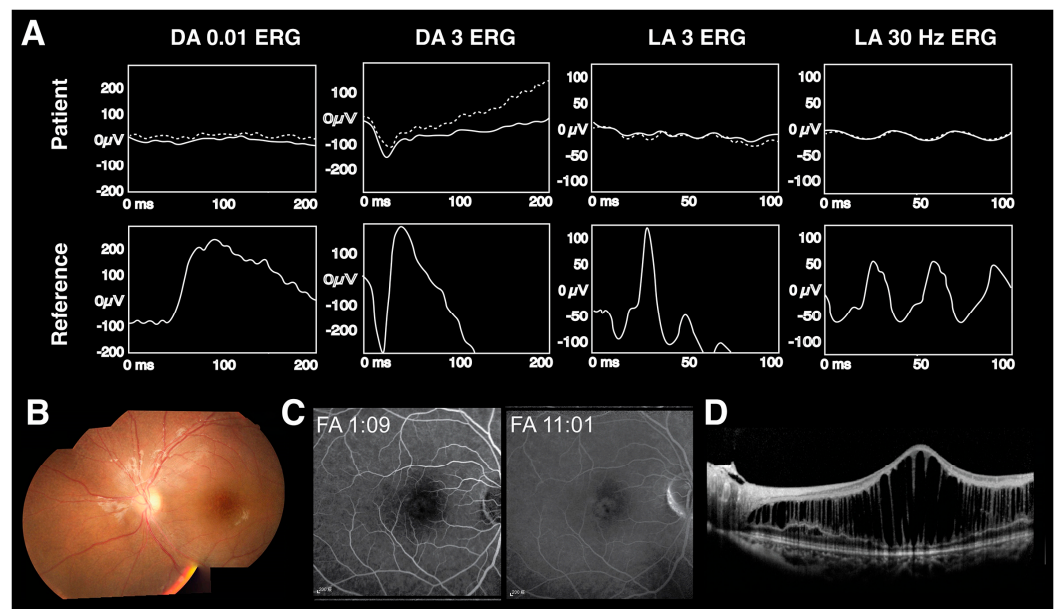


**Figure 5.** The typical findings from X-linked retinoschisis (XLRs) in a Taiwanese cohort [40]. (A) ERG results revealing electronegative DA 3 ERG and reduced scotopic response. (B) Spoke-wheel-like pattern at the macula. (C) Fluorescein angiography (FA) shows non-leaking cystoid macular edema (CME). (D) Schisis and increased thickness at the macula.

### 3.4. Management and Prognosis

In terms of managing XLRS patients, there are positive findings from the use of carbonic anhydrase inhibitors (CAIs) and preimplantation genetic diagnosis to conceive a sibling of an XLRS patient [40], but gene therapies have not shown promising results.

CAIs have been used to treat schisis or CME, which is achieved by modulating carbonic anhydrase IV receptors on the RPE membrane or by enhancing fluid transport [44,45]. However, the effectiveness of CAIs varies, and reports suggest that their impact is more visible in improving central foveal thickness and less so in improving visual acuity [40,46,47].

The eye is an ideal target for gene delivery systems to restore functional retinal proteins because of its accessibility and immune-privileged status [48]. However, while the AAV vector-based gene therapy drug was successful in treating patients with confirmed biallelic *RPE65* mutation-associated Leber Congenital Amaurosis (LCA) and was approved by the FDA in 2017 [35], clinical trials of gene therapy on XLRS patients have shown unpromising results. There have been two clinical trials for gene therapies administered through intravitreal injection and mediated by AAV, of which one trial (ClinicalTrials.gov: NCT02416622) was stopped due to a high number of inflammatory adverse events, such as vitritis, while the other (ClinicalTrials.gov: NCT02317887) did not show significant improvements in a preliminary report [49]. A new technique has been developed to enhance previous trials' effectiveness called "AAV.SPR", and this uses AAV capsids that can spread beyond the injection site under the retina, ensuring the safe delivery of the *RS1* gene to photoreceptors in the central retina/foveal region [50]. The United States Food and Drug Administration (FDA) has recently approved a clinical trial for XLRS patients that will utilize the AAV.SPR delivery system and be administered through a subretinal injection (ClinicalTrials.gov: NCT05878860) [51].

To conclude, in order to investigate the accurate efficacy of CAIs or *RS1*-gene therapy on XLRS, larger prospective randomized trials involving younger participants with less severe retinal structural changes are necessary.

## 4. CRX-Related Cone–Rod Dystrophy

### 4.1. Pathophysiology

The *CRX* gene is located in the cone–rod homeobox gene, involving the development and maintenance of photoreceptors [52]. Pathogenic mutations in the *CRX* gene may give rise to a wide spectrum of retinal diseases including progressive cone–rod dystrophy [53]. Although the retinal expression of *CRX* is limited to photoreceptors, this dysfunction may result from faulty photoreceptor communication with second-order retinal neurons [54].

### 4.2. Clinical Presentation

Patients with *CRX*-related progressive cone–rod dystrophy inherit in an AD manner, with onsets occurring at adulthood [55]. The phenotype and penetrance widely vary [56]. Since the cones are more affected than rods, patients present with difficulty in visual acuity, central vision, color discrimination, or photophobia and show maculopathy in fundus imaging. As the disease progresses, rod dysfunction becomes more apparent, leading to loss of the peripheral visual field and nyctalopia.

### 4.3. ERG Findings

In addition to the ERG pattern of cone–rod dystrophy, where photopic ERG responses are more affected than scotopic responses, patients with *CRX*-related cone–rod dystrophy typically present with electronegative waveforms in DA 3 or 10 ERG tests, consistent with the dysfunction site between photoreceptors and second-order retinal neurons [57]. The electronegative ERG feature is a highly sensitive diagnostic marker in patients with *CRX*-related cone–rod dystrophy [57]. It helps rule out *CRX* retinopathy in family members, as this may be the only clinical abnormality detected in asymptomatic patients [58]. Figure 6 shows the fundus and ERG pattern in a case of *CRX*-related cone–rod dystrophy.

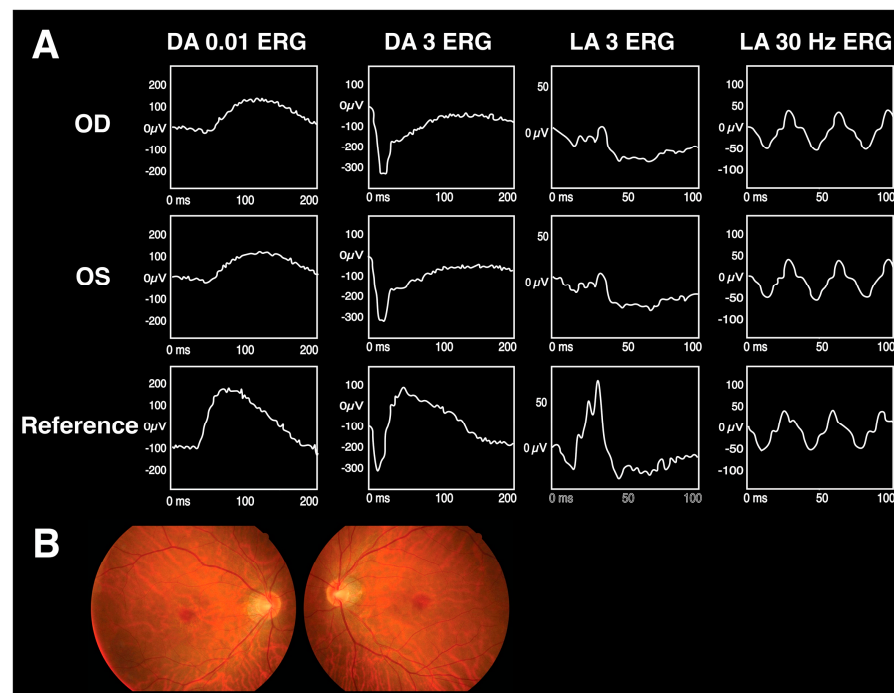


**Figure 6.** The findings on CXR-related cone-rod dystrophy in a Taiwanese case. (A) ERG report revealing reduced scotopic response and electronegative DA 3 ERG. (B) Fundus examination.

#### 4.4. Other Genes with These Features

Similar to the *CRX* mutation, there are other gene mutations that cause AD-inherited progressive cone-rod dystrophy and show the electronegative scotopic response to strong light stimuli, including the *RAX2*, *GUCY2D*, and *PRPH2* genes.

The *RAX2* gene, previously named *QRX* or *RAXL1*, has a sequence homologous to the *CRX* gene wherein the two genes encode proteins to interact synergistically to be involved in transcription in the retina's outer and inner nuclear layers [59]. Mutations in the *GUCY2D* gene cause defects in photoreceptor synaptic transmission to second-order neurons, consistent with the electronegative waveform [60]. *PRPH2* mutations can give rise to not only AD-inherited progressive cone-rod dystrophy but also macula dystrophy and rod-cone dystrophy [61,62]. The gene encodes peripherin, a transmembrane protein in the outer segments of the photoreceptors, and contributes to the site's morphogenesis, stabilization, and renewal [55,56].

## 5. Fundus Albipunctatus

### 5.1. Pathophysiology

Fundus albipunctatus, an autosomal recessive disease, is caused by mutations in the *RDH5* gene, which encodes retinol dehydrogenase 5, an enzyme expressed at RPE [63]. It involves the visual cycle, which oxidates 11-cis-retinol into 11-cis-retinal, to help recycle the chromophore back to its original form before receiving light stimuli. The interruption of this process restricts the photopigment turnover and leads to reduced lipofuscin formation, which is derived from the photoreceptor outer segments debris. The process is displayed in Figure 2.

### 5.2. Clinical Presentation

Fundus albipunctatus is classified under the disease category of CSNB due to its characteristic of non-progressive night blindness. Distinguishing this disease from other types of CSNB involves observing abnormal findings in the fundus and noting the improvement of scotopic ERG responses after an extended period of dark adaptation due to the photopigment's slow regeneration rate.



As the name suggests, fundus imaging shows retinal white-yellowish dots at the posterior pole, sparing the fovea. Using fundus autofluorescence (FAF), lipofuscin accumulation in the patient's RPE can be mapped in vivo [64], and this shows hypo-FAF signals [65]. Infrared scanning laser ophthalmoscopy (IR) provides detailed images of subretinal lesions and displays hyperreflective spots [66].

### 5.3. ERG Findings

The ERG patterns of fundus albipunctatus are characteristic of the recovery of the scotopic response after prolonged scotopic adaptation [67]. Electronegative ERG results in response to a bright flash may occur due to the dark-adapted cone system being exposed without a normal rod function [65]. They should not be assumed to reflect inner retinal rod system dysfunction. Figure 7 depicts the fundus imaging, FAF, and ERG examinations of a patient with fundus albipunctatus.

### 5.4. Differential Diagnosis

In addition to being found in patients with fundus albipunctatus, white retinal dots can also be observed in those with retinitis punctata albescens (RPA) [68] caused by *RLBP1* mutations and in cases of benign retinal flecks. However, the absence of any abnormalities in ERG can differentiate benign retinal flecks from other conditions. To distinguish between RPA and fundus albipunctatus, it is noteworthy that abnormal ERG patterns in RPA do not improve after extended scotopic adaptation, and the symptoms of nyctalopia and restricted visual field worsen over time [69].

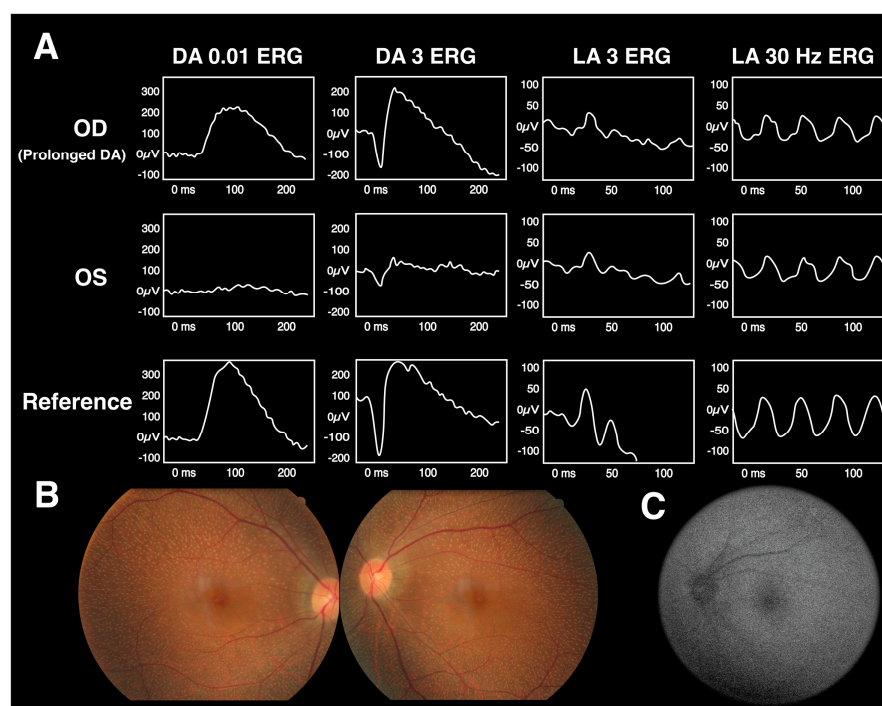


**Figure 7.** The findings on fundus albipunctatus in a Taiwanese case [66]. (A) ERG results revealing recovery of the DA 3 ERG response after prolonged scotopic adaptation. (B) Fundus examination with retinal white dots at the posterior pole, sparing the fovea. (C) Fundus autofluorescence (FAF) showing mottling hypo-autofluorescent signals.

## 6. Enhanced S-Cone Syndrome (ESCS), or Goldmann–Favre Syndrome

### 6.1. Pathophysiology

Enhanced S-cone syndrome (ESCS), also known as Goldmann–Favre syndrome, is an autosomal recessively inherited retinal dystrophy caused by pathogenic mutations in the orphan nuclear receptor transcription factor (*NR2E3*) gene, which is responsible for the

suppression of cone-specific genes in rods during embryogenesis [70]. *NR2E3* mutations result in excess S-cones, and the decreased number of rods in and clumping of S-cones lead to retinal dysplasia and degeneration.

### 6.2. Clinical Presentation

Patients with ESCS present with nyctalopia, variable visual acuity loss, and constricted field of vision [71]. The fundus in ESCS patients may show round pigment clumping along the vascular arcades in the mid-periphery of the retina in older patients or retinal white dots in younger patients [72–74]. OCT reveals cystoid macular edema [75,76], which can be confirmed to be non-leaking by using FA. The rosette-like lesions from the RPE in OCT correspond to hyper-autofluorescent signals resulting from resident microglia infiltration [77,78].

### 6.3. ERG Findings

Patients with ESCS exhibit three distinct ERG features. Firstly, the cone-dominated retina causes the DA 0.01 ERG results to be extinguished. Secondly, waveforms in DA 3 or 10 ERG reports are similar to those in LA 3 ERG in shape as both are light-stimulated responses from mere cones, not rods. Thirdly, the LA 3 ERG a-wave shows increased amplitudes due to having an increased number of cones, with amplitudes larger than those of the LA 30 Hz ERG wave. Moreover, the presence of excess S-cones can be verified by observing an elevated signal in S-cone ERG. Figure 8 demonstrates the fundus and ERG findings on ESCS patients.

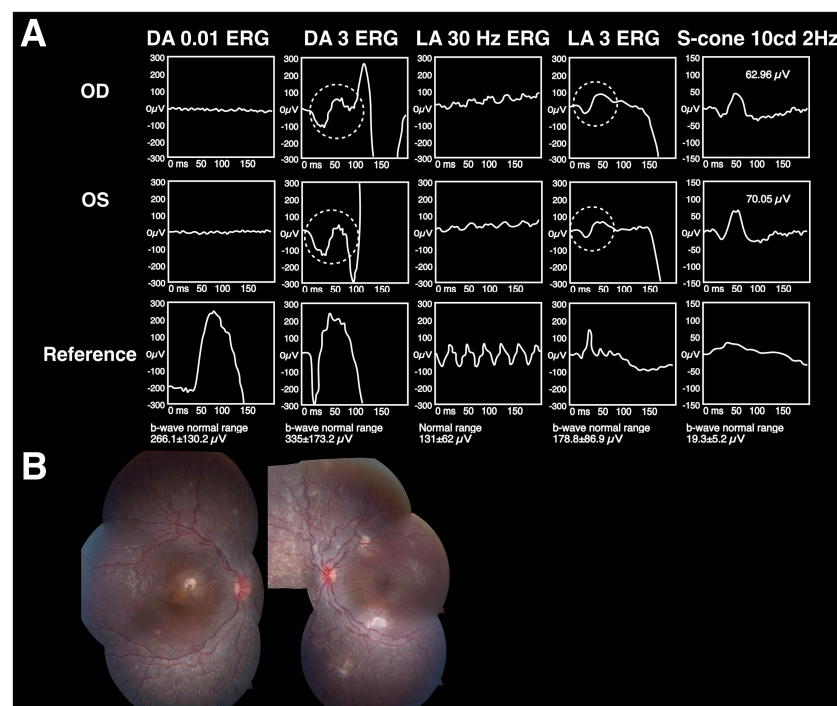


**Figure 8.** The findings on a patient with Enhanced S-cone syndrome (ESCS), also known as Goldmann–Favre syndrome [77]. (A) Three distinct ERG features, including extinguished DA 0.1 ERG, similar waveforms in DA 3 or 10 ERG reports and LA 3 ERG, and a larger a-wave in LA 3 ERG than in LA 30 Hz ERG. Moreover, excess S-cones can be verified by observing an elevated signal in S-cone ERG. (B) Fundus examination revealing retinal white dots.

### 6.4. Differential Diagnosis

Both ESCS and RP can manifest with pigmentary changes in the fundus. To differentiate, the pigmentary changes in ESCS are round and distributed in the mid-periphery of the retina, while those of RP appear as bone spicules [79,80].

## 7. Cone Dystrophy with Supernormal Rod Response (CDSRR)

### 7.1. Pathophysiology

Cone dystrophy with supernormal rod response (CDSRR) is an autosomal recessively inherited retinal dystrophy caused by pathogenic mutations in the potassium voltage-gated channel modifier subfamily V member 2 (*KCNV2*) gene. This gene is expressed in rods and cones and is responsible for the assembly of potassium voltage-gated channels [81].

### 7.2. Clinical Presentation

Dysfunctional cones cause reduced central visual acuity and color vision while abnormal rods lead to photophobia and nyctalopia [82]. These symptoms typically appear within the first two decades of life [83]. Fundus imaging is limited in its ability to diagnose CDSRR due to the possibility of non-specific appearances including maculopathy. Instead, a CDSRR diagnosis is based on identifying distinctive ERG findings due to *KCNV2* mutations.

### 7.3. ERG Findings

Patients with CDSRR have two distinguishable features. Firstly, the photopic response is reduced and delayed to a great extent, consistent with universal cone dysfunction. Secondly, DA 0.01 ERG is reduced and significantly delayed while DA 3.0 ERG showed a disproportionately augmented b-wave, or a “supernormal rod response” manifests. Testing all patients with these two characteristic ERG features is recommended since the *KCNV2* gene has two exons, making direct sequencing affordable [84].

### 7.4. Differential Diagnosis

In patients with hydroxychloroquine (HCQ) retinopathy, the toxicity initially affects the photoreceptor and then progresses to the RPE cells. The bull’s eye maculopathy in the fundus imaging of CDSRR patients may be mistaken as HCQ retinopathy, but OCT, FAF, and ERG can help distinguish the two causes [85]. It should be noted that a history of taking HCQ does not rule out the differential diagnosis of CDSRR [84]. Figure 9 displays the fundus and ERG findings on a patient with CDSRR, initially mistaken for HCQ retinopathy.

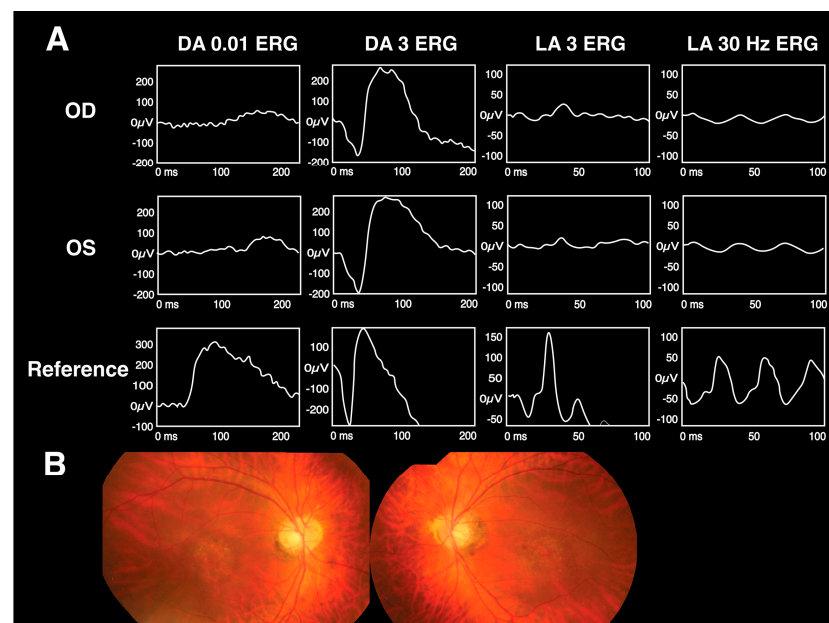


**Figure 9.** The findings on a patient with cone dystrophy with supernormal rod response (CDSRR), who was initially mistaken as having HCQ retinopathy [84]. The distinct ERG patterns helped pinpoint the candidate gene for a definite diagnosis. (A) ERG report showing a supernormal rod response to bright flash intensity in the setting of cone and rod dystrophy. (B) Fundus imaging showing symmetric atrophic lesion at the central macula in both eyes.

In severe cases of HCQ retinopathy, OCT may exhibit a flying saucer sign, indicating the loss of parafoveal structure [86]. Additionally, FAF may display parafoveal hyperautofluorescent with or without parafoveal dark areas [87]. While ERG patterns may vary, they do not exhibit supernormal rod response to bright stimuli in the presence of reduced cone and rod response.

## 8. Challenges and Limitations of ERG in Diagnosis

### 8.1. Technical Considerations

In clinical settings where IRDs are being investigated, mydriasis or ophthalmic examinations with bright illumination are frequently conducted. There are certain technical concerns to consider if ERG is recorded following these examinations [7].

To begin with, mydriasis is not mandatory as per the latest ISCEV-standard ERG protocol as long as the reference ranges are used with the same settings. Nevertheless, if mydriasis is used, it is necessary to document the pupil diameter before and after ERG recording.

Second, following intensely illuminated ophthalmic examinations, it is essential to recover in a well-lit area for at least 30 min before performing an ERG recording to obtain accurate data.

### 8.2. Variability and Standardization of ERG Protocols

For consistent ERG recording across different subjects, visits, and laboratories, it is essential to standardize ERG protocols based on the ISCEV's standard protocol. It is recommended to establish reference values specific to each laboratory using subjects with similar demographics to the patient population. ERG for infants under 6 months of age must be approached cautiously as their readings may be unclear or show lower amplitudes and longer peak times [7]. In general, photopic ERG tests in infants mature by 3 months, while scotopic ERG tests mature by 6 months.

The ERG results of patients with refractive errors or comorbidities should be interpreted with caution. In myopic patients, the b-wave amplitudes were found to be lower than in patients without refractive errors, with scotopic responses being more affected than photopic responses. This effect is more pronounced in patients with myopic-related structural retinal changes [88–90]. Patients with glaucoma or optic nerve diseases may exhibit reduced b-wave amplitudes in DA 0.01 ERG, but they may have larger amplitudes for the photopic negative response, that is, the negative waveform following the b-wave. However, the diagnostic value of ffERG, which is based on a- and b-waves, remains unaffected and is still crucial in diagnosing various eye diseases.

The laboratory-specific reference values should be included in the ERG reports of patients to facilitate interpretation. Additionally, it is useful to document the testing time, pupil diameters, and the type of the recording electrodes used. Specifically, the type of the recording electrodes is important to note, as contact-lens-recording electrodes tend to show higher ERG wave amplitudes compared to lower-eyelid-skin electrodes [91].

### 8.3. Importance of Integrating Clinical Findings and Multimodal Imaging with ERG

Genetic testing is essential for managing IRD patients. It aids in providing an accurate diagnosis, predicting the prognosis, communicating the risk of inheritance, and determining eligibility for gene-based therapies or clinical trials.

In such cases, targeted sequencing guided by clinical assessment is preferred over whole-genome sequencing (WGS) or whole-exome sequencing (WES) approaches for several reasons [92]. Compared to WGS, targeted sequencing requires less cost, data storage, and effort to analyze incidental findings that are not related to the presenting disease. Alternatively, unlike WES, targeted sequencing is capable of detecting deep intronic mutations, which could be the root causes of certain IRDs [93,94].

Performing the target sequencing of genes related to suspected IRDs requires precise clinical assessment, which highlights the importance of integrating clinical findings,

multimodal imaging, and ERG reports. Personal and family medical history should be obtained when evaluating people with suspected IRDs. This should include any symptoms of rod (such as nyctalopia or peripheral visual field loss) or cone dysfunction (such as impaired central or color vision or photophobia), the age at which symptoms began and how they progressed, and any medication usage. Multimodal imaging is then used to evaluate structural changes. To clarify, fundus imaging can distinguish between different types of CSNBs. OCT allows for a cross-sectional view of the retinal layers, such as in the detection of retinal schisis in XLRs patients. Additionally, hypo-autofluorescent signals can indicate lower lipofuscin in the RPE, consistent with fundus albipunctatus. Finally, ERG tests are utilized to identify the specific layer of dysfunctional retinal cells that plays a critical role in differential diagnosis.

## 9. Conclusions

### 9.1. Summary of Findings

IRDs are a clinically and genetically heterogeneous group of diseases with emerging therapeutics signaling the need for precise diagnosis. IRDs primarily affect the rod or cone photoreceptors or inner retinal neuronal layers, where ERG identifies the defective region and guides genetic tests for confirmative diagnosis.

An electronegative waveform in scotopic ERG, which is a lower amplitude of b-wave compared to that of the a-wave, indicates inner retinal diseases. These include complete, incomplete, and Riggs-type CSNB, XLRs, and cone-rod dystrophies related to *CRX*, *GUCY2D*, *PRPH2*, or *RAX2*. Electronegative waveforms are not typical of fundus albipunctatus, ESCS, and CDSRR, but they have their own distinctive ERG patterns.

This review provides a guide for diagnosing IRDs that exhibit specific ERG features. Table 2 summarizes the symptoms, multimodal imaging findings, inheritance patterns, and ERG features of these IRDs. This information guides the clinical assessment and further pinpoints the specific genes to be tested for diagnosis.

### 9.2. Clinical Implications and the Unique Role of ERG in Diagnosing Select Retinal Disorders

ERG is essential throughout stages of IRD management, including clinical assessment for guiding genomic tests and tracking visual function over time [95].

Precise clinical assessments of IRDs are important because they are crucial for both disease diagnosis, such as in aiding the interpretation of genetic variants of uncertain significance [96], and for research purposes, like in segregation studies of candidate genetic variants [97]. Precise clinical assessments of IRDs rely on ERG rather than just imaging studies. While fundus imaging is useful for studying anatomical pathologies, stable fixation is necessary for high-quality images [98,99]. Conversely, ERG examines functional dysfunctions in retinal cells that may occur before ophthalmoscopic changes and does not require as much stable fixation during recording as other electrophysiology techniques [7]. These features render ERG a crucial tool for accurately diagnosing IRDs, particularly in younger patients, as young patients with IRDs are more susceptible to the onset of these diseases, may have nystagmus affecting fundus image quality, and may benefit from early interventions.

ERG offers direct retinal response measurements, with a broad application and non-invasive nature, but it is limited by variability and requires further genetic testing for definite diagnosis. In contrast, NGS provides comprehensive gene screening with high sensitivity, but it is cost-intensive and demands complex data interpretation. Microarray analysis, being high-throughput as well but more affordable than NGS, can miss rare variants and hinges on known genetic data. In conclusion, while ERG furnishes essential functional insights, its diagnostic capacity is augmented when paired with molecular techniques like NGS and microarray. This combined approach enriches our understanding and diagnosis of inherited retinal dystrophies.



### 9.3. Limitations and Future Research Advancements in ERG Applications

There are potential limitations that may impede the broad acceptance of ERG in diagnosing IRDs. Advanced ERG devices could be expensive, which might limit their accessibility, especially in resource-limited settings. The specificity and sophistication of ERG demand expertise, which could be a barrier in places with a shortage of trained professionals. Some medications and substances, including alcohol or sedatives, can affect the ERG waveform [100]. A comprehensive medical history and understanding of potential interactions are essential for accurate interpretation.

The technology of ERG has advanced in the areas of portable devices and the use of machine learning for analysis and modeling [101]. Handheld ERG technology provides portable and accessible recording that would help identify IRDs in clinical settings that need further referral to specialized centers and for uncooperative or supine-positioned infants. This technology has produced results consistent with standard systems in pediatric patients [102]. Additionally, reports of handheld ERG devices are being used to diagnose specific IRDs [103].

Artificial intelligence (AI) has been widely applied to healthcare systems, including in the field of ERG. Studies showed that machine learning could help classify ERG features in patients with IRD, other ocular diseases, or psychiatric diseases [104–106]. For decades, ERG has played a vital role in studying the retina. Although retinal imaging has improved, ERG remains relevant for quantitatively assessing retinal cells in vivo. With advancing technology and AI-assisted analyses, testing for retinal diseases is becoming more accessible and informative.

**Author Contributions:** Conceptualization, T.-H.Y., E.Y.-C.K. and N.-K.W.; writing—original draft preparation, T.-H.Y., E.Y.-C.K. and N.-K.W.; writing—review and editing, T.-H.Y., E.Y.-C.K., P.-H.L. and J.A.S.; visualization, T.-H.Y. and P.-L.W.; supervision, N.-K.W.; project administration, T.-H.Y., E.Y.-C.K. and N.-K.W.; funding acquisition, N.-K.W. All authors have read and agreed to the published version of the manuscript.

**Funding:** Nan-Kai Wang and his laboratory are supported by the National Institute of Health (R01EY031354, P30EY019007), Vagelos College of Physicians & Surgeons (VP&S) Grants Gerstner Philanthropies, and in part, by an Unrestricted Grant to the Department of Ophthalmology, Columbia University, from Research to Prevent Blindness, New York, NY. The content is solely the responsibility of the authors and does not necessarily represent the official views of the National Institutes of Health. The APC was waived.

**Institutional Review Board Statement:** The study was conducted in accordance with the Declaration of Helsinki, and approved by the Institutional Review Board of Chang Gung Medical Foundation (IRB No. 201601569B0C602).

**Informed Consent Statement:** Informed consent was obtained from all subjects involved in the study.

**Data Availability Statement:** Not applicable.

**Acknowledgments:** The authors extend their gratitude to the Retinal Imaging and Electrophysiology Technicians at the Department of Ophthalmology, Chang Gung Memorial Hospital, in both Linkou and Taipei, for their valuable technical support.

**Conflicts of Interest:** The authors declare no conflict of interest. The funders had no role in the design of the study; in the collection, analysis, or interpretation of data; in the writing of the manuscript; or in the decision to publish the results.

## References

1. National Human Genome Research Institute. The Cost of Sequencing a Human Genome. Available online: <https://www.genome.gov/about-genomics/fact-sheets/Sequencing-Human-Genome-cost> (accessed on 28 May 2023).
2. Vickers, A.J.; Van Calster, B.; Steyerberg, E.W. Net benefit approaches to the evaluation of prediction models, molecular markers, and diagnostic tests. *BMJ* **2016**, *352*, i6. [[CrossRef](#)] [[PubMed](#)]
3. Bertozzi, S.; Londero, A.P.; Xholli, A.; Azioni, G.; Di Vora, R.; Paudice, M.; Bucimazza, I.; Cedolini, C.; Cagnacci, A. Risk-Reducing Breast and Gynecological Surgery for BRCA Mutation Carriers: A Narrative Review. *J. Clin. Med.* **2023**, *12*, 1422. [[CrossRef](#)] [[PubMed](#)]

4. Purves, D.; Augustine, G.J.; Fitzpatrick, D. Neuroscience. In *Anatomical Distribution of Rods and Cones*, 2nd ed.; Sinauer Associates: Sunderland, MA, USA, 2001.
5. Lamb, T.D. Photoreceptor physiology and evolution: Cellular and molecular basis of rod and cone phototransduction. *J. Physiol.* **2022**, *600*, 4585–4601. [[CrossRef](#)] [[PubMed](#)]
6. Ichinose, T.; Habib, S. ON and OFF Signaling Pathways in the Retina and the Visual System. *Front. Ophthalmol.* **2022**, *2*, 989002. [[CrossRef](#)] [[PubMed](#)]
7. Robson, A.G.; Frishman, L.J.; Grigg, J.; Hamilton, R.; Jeffrey, B.G.; Kondo, M.; Li, S.; McCulloch, D.L. ISCEV Standard for full-field clinical electroretinography (2022 update). *Doc. Ophthalmol.* **2022**, *144*, 165–177. [[CrossRef](#)] [[PubMed](#)]
8. Audo, I.; Robson, A.G.; Holder, G.E.; Moore, A.T. The negative ERG: Clinical phenotypes and disease mechanisms of inner retinal dysfunction. *Surv. Ophthalmol.* **2008**, *53*, 16–40. [[CrossRef](#)] [[PubMed](#)]
9. Jiang, X.; Mahroo, O.A. Negative electroretinograms: Genetic and acquired causes, diagnostic approaches and physiological insights. *Eye* **2021**, *35*, 2419–2437. [[CrossRef](#)] [[PubMed](#)]
10. Vercio, A.; Chalam, K.V.; Winter, T. Typical electronegative electroretinography and nyctalopia as a presenting feature of systemic malignant melanoma. *Int. Med. Case Rep. J.* **2019**, *12*, 265–276. [[CrossRef](#)]
11. Chiang, T.K.; White, K.M.; Kurup, S.K.; Yu, M. Use of Visual Electrophysiology to Monitor Retinal and Optic Nerve Toxicity. *Biomolecules* **2022**, *12*, 1390. [[CrossRef](#)]
12. Kim, H.M.; Park, K.H.; Woo, S.J. Correlation of electroretinography components with visual function and prognosis of central retinal artery occlusion. *Sci. Rep.* **2020**, *10*, 12146. [[CrossRef](#)]
13. Saker, S.; Morales, M.; Jhittay, H.; Wen, Y.; Amoaku, W. Electrophysiological and microperimetry changes in vitamin A deficiency retinopathy. *Doc. Ophthalmol.* **2015**, *130*, 231–240. [[CrossRef](#)]
14. Tsang, S.H.; Sharma, T. Congenital Stationary Night Blindness. *Adv. Exp. Med. Biol.* **2018**, *1085*, 61–64. [[CrossRef](#)] [[PubMed](#)]
15. De Silva, S.R.; Arno, G.; Robson, A.G.; Fakin, A.; Pontikos, N.; Mohamed, M.D.; Bird, A.C.; Moore, A.T.; Michaelides, M.; Webster, A.R.; et al. The X-linked retinopathies: Physiological insights, pathogenic mechanisms, phenotypic features and novel therapies. *Prog. Retin. Eye Res.* **2021**, *82*, 100898. [[CrossRef](#)] [[PubMed](#)]
16. Morgans, C.W.; Brown, R.L.; Duvoisin, R.M. TRPM1: The endpoint of the mGluR6 signal transduction cascade in retinal ON-bipolar cells. *Bioessays* **2010**, *32*, 609–614. [[CrossRef](#)] [[PubMed](#)]
17. Morgans, C.W.; Zhang, J.; Jeffrey, B.G.; Nelson, S.M.; Burke, N.S.; Duvoisin, R.M.; Brown, R.L. TRPM1 is required for the depolarizing light response in retinal ON-bipolar cells. *Proc. Natl. Acad. Sci. USA* **2009**, *106*, 19174–19178. [[CrossRef](#)] [[PubMed](#)]
18. Schneider, F.M.; Mohr, F.; Behrendt, M.; Oberwinkler, J. Properties and functions of TRPM1 channels in the dendritic tips of retinal ON-bipolar cells. *Eur. J. Cell Biol.* **2015**, *94*, 420–427. [[CrossRef](#)] [[PubMed](#)]
19. Pearring, J.N.; Bojang, P., Jr.; Shen, Y.; Koike, C.; Furukawa, T.; Nawy, S.; Gregg, R.G. A role for nyctalopin, a small leucine-rich repeat protein, in localizing the TRP melastatin 1 channel to retinal depolarizing bipolar cell dendrites. *J. Neurosci.* **2011**, *31*, 10060–10066. [[CrossRef](#)]
20. Hasan, N.; Pangen, G.; Cobb, C.A.; Ray, T.A.; Nettesheim, E.R.; Ertel, K.J.; Lipinski, D.M.; McCall, M.A.; Gregg, R.G. Presynaptic Expression of LRIT3 Transsynaptically Organizes the Postsynaptic Glutamate Signaling Complex Containing TRPM1. *Cell Rep.* **2019**, *27*, 3107–3116.e3103. [[CrossRef](#)]
21. Kim, A.H.; Liu, P.K.; Chang, Y.H.; Kang, E.Y.; Wang, H.H.; Chen, N.; Tseng, Y.J.; Seo, G.H.; Lee, H.; Liu, L.; et al. Congenital Stationary Night Blindness: Clinical and Genetic Features. *Int. J. Mol. Sci.* **2022**, *23*, 14965. [[CrossRef](#)]
22. Gravier, N. [Etiological assessment of a nystagmus in childhood]. *J. Fr. Ophthalmol.* **2018**, *41*, 868–878. [[CrossRef](#)]
23. Blair, K.; Cibis, G.; Gulani, A.C. Amblyopia. In *StatPearls*; StatPearls Publishing: Treasure Island, FL, USA, 2023. Available online: <https://pubmed.ncbi.nlm.nih.gov/28613640/> (accessed on 1 August 2023).
24. MacDonald, I.M.; Hoang, S.; Tuupainen, S. X-Linked Congenital Stationary Night Blindness. In *GeneReviews*<sup>®</sup>; Adam, M.P., Mirzaa, G.M., Pagon, R.A., Wallace, S.E., Bean, L.J.H., Gripp, K.W., Amemiya, A., Eds.; University of Washington: Seattle, WA, USA, 1993.
25. Kim, H.M.; Joo, K.; Han, J.; Woo, S.J. Clinical and Genetic Characteristics of Korean Congenital Stationary Night Blindness Patients. *Genes* **2021**, *12*, 789. [[CrossRef](#)] [[PubMed](#)]
26. Marmor, M.F.; Zeitz, C. Riggs-type dominant congenital stationary night blindness: ERG findings, a new GNAT1 mutation and a systemic association. *Doc. Ophthalmol.* **2018**, *137*, 57–62. [[CrossRef](#)] [[PubMed](#)]
27. Hung, W.C.; Cheng, H.C.; Wang, A.G. Melanoma-associated retinopathy with anti-TRPM1 autoantibodies showing concomitant Off-bipolar cell dysfunction. *Doc. Ophthalmol.* **2022**, *145*, 263–270. [[CrossRef](#)] [[PubMed](#)]
28. Huang, W.C.; Liu, P.K.; Wang, N.K. Electroretinogram (ERG) to Evaluate the Retina in Cases of Retinitis Pigmentosa (RP). *Methods Mol. Biol.* **2023**, *2560*, 111–122. [[CrossRef](#)] [[PubMed](#)]
29. Dryja, T.P.; McGee, T.L.; Berson, E.L.; Fishman, G.A.; Sandberg, M.A.; Alexander, K.R.; Derlacki, D.J.; Rajagopalan, A.S. Night blindness and abnormal cone electroretinogram ON responses in patients with mutations in the GRM6 gene encoding mGluR6. *Proc. Natl. Acad. Sci. USA* **2005**, *102*, 4884–4889. [[CrossRef](#)] [[PubMed](#)]
30. Nakamura, M.; Ito, S.; Piao, C.H.; Terasaki, H.; Miyake, Y. Retinal and optic disc atrophy associated with a CACNA1F mutation in a Japanese family. *Arch. Ophthalmol.* **2003**, *121*, 1028–1033. [[CrossRef](#)]
31. Scalabrino, M.L.; Boye, S.L.; Fransen, K.M.; Noel, J.M.; Dyka, F.M.; Min, S.H.; Ruan, Q.; De Leeuw, C.N.; Simpson, E.M.; Gregg, R.G.; et al. Intravitreal delivery of a novel AAV vector targets ON bipolar cells and restores visual function in a mouse model of complete congenital stationary night blindness. *Hum. Mol. Genet.* **2015**, *24*, 6229–6239. [[CrossRef](#)]

32. Varin, J.; Bouzidi, N.; Dias, M.M.S.; Pugliese, T.; Michiels, C.; Robert, C.; Desrosiers, M.; Sahel, J.A.; Audo, I.; Dalkara, D.; et al. Restoration of mGluR6 Localization Following AAV-Mediated Delivery in a Mouse Model of Congenital Stationary Night Blindness. *Investig. Ophthalmol. Vis. Sci.* **2021**, *62*, 24. [CrossRef]
33. Varin, J.; Bouzidi, N.; Gauvain, G.; Joffrois, C.; Desrosiers, M.; Robert, C.; De Sousa Dias, M.M.; Neullé, M.; Michiels, C.; Nassisi, M.; et al. Substantial restoration of night vision in adult mice with congenital stationary night blindness. *Mol. Ther. Methods Clin. Dev.* **2021**, *22*, 15–25. [CrossRef]
34. Miyadera, K.; Santana, E.; Roszak, K.; Iffrig, S.; Visel, M.; Iwabe, S.; Boyd, R.F.; Bartoe, J.T.; Sato, Y.; Gray, A.; et al. Targeting ON-bipolar cells by AAV gene therapy stably reverses LRIT3-congenital stationary night blindness. *Proc. Natl. Acad. Sci. USA* **2022**, *119*, e2117038119. [CrossRef]
35. Chiu, W.; Lin, T.Y.; Chang, Y.C.; Isahwan-Ahmad Mulyadi Lai, H.; Lin, S.C.; Ma, C.; Yarmishyn, A.A.; Lin, S.C.; Chang, K.J.; Chou, Y.B.; et al. An Update on Gene Therapy for Inherited Retinal Dystrophy: Experience in Leber Congenital Amaurosis Clinical Trials. *Int. J. Mol. Sci.* **2021**, *22*, 4534. [CrossRef] [PubMed]
36. Holmes, J.M.; Lazar, E.L.; Melia, B.M.; Astle, W.F.; Dagi, L.R.; Donahue, S.P.; Frazier, M.G.; Hertle, R.W.; Repka, M.X.; Quinn, G.E.; et al. Effect of age on response to amblyopia treatment in children. *Arch. Ophthalmol.* **2011**, *129*, 1451–1457. [CrossRef] [PubMed]
37. Molday, R.S.; Kellner, U.; Weber, B.H. X-linked juvenile retinoschisis: Clinical diagnosis, genetic analysis, and molecular mechanisms. *Prog. Retin. Eye Res.* **2012**, *31*, 195–212. [CrossRef] [PubMed]
38. Orès, R.; Mohand-Said, S.; Dhaenens, C.M.; Antonio, A.; Zeitz, C.; Augstburger, E.; Andrieu, C.; Sahel, J.A.; Audo, I. Phenotypic Characteristics of a French Cohort of Patients with X-Linked Retinoschisis. *Ophthalmology* **2018**, *125*, 1587–1596. [CrossRef] [PubMed]
39. Xiao, S.; Sun, W.; Xiao, X.; Li, S.; Luo, H.; Jia, X.; Ouyang, J.; Li, X.; Wang, Y.; Jiang, Y.; et al. Clinical and genetic features of retinoschisis in 120 families with RS1 mutations. *Br. J. Ophthalmol.* **2023**, *107*, 367–372. [CrossRef] [PubMed]
40. Wang, N.K.; Liu, L.; Chen, H.M.; Tsai, S.; Chang, T.C.; Tsai, T.H.; Yang, C.M.; Chao, A.N.; Chen, K.J.; Kao, L.Y.; et al. Clinical presentations of X-linked retinoschisis in Taiwanese patients confirmed with genetic sequencing. *Mol. Vis.* **2015**, *21*, 487–501. [PubMed]
41. Parra, M.M.; Hartnett, M.E. Vitreous hemorrhage in X-linked retinoschisis. *Am. J. Ophthalmol. Case Rep.* **2022**, *25*, 101395. [CrossRef]
42. Greig, L.C.; Gutierrez, K.G.; Oh, J.K.; Levi, S.R.; Korot, E.; Tsang, S.H.; Mahajan, V.B. Multimodal imaging reveals retinoschisis masquerading as retinal detachment in patients with choroideremia. *Am. J. Ophthalmol. Case Rep.* **2022**, *26*, 101543. [CrossRef]
43. Tondelli, N.N.; Mencaroni, B.M.; Lemos, C.M.B.; Rocha de Sousa, J.; Sandoval Barbosa, G.C.; Gomes, A.M.V.; da Palma, M.M. A patient with X-linked retinoschisis and exudative retinal detachment associated with a pathogenic hemizygous variant c.304c>T in RS1. *Ophthalmic Genet.* **2022**, *43*, 871–875. [CrossRef]
44. Wolfensberger, T.J.; Mahieu, I.; Jarvis-Evans, J.; Boulton, M.; Carter, N.D.; Nógrádi, A.; Hollande, E.; Bird, A.C. Membrane-bound carbonic anhydrase in human retinal pigment epithelium. *Investig. Ophthalmol. Vis. Sci.* **1994**, *35*, 3401–3407.
45. Wolfensberger, T.J. The role of carbonic anhydrase inhibitors in the management of macular edema. *Doc. Ophthalmol.* **1999**, *97*, 387–397. [CrossRef] [PubMed]
46. Schmitt, M.A.; Wang, K.; DeBenedictis, M.J.; Traboulsi, E.I. Topical carbonic anhydrase inhibitors in the long-term treatment of juvenile X-linked retinoschisis. *Retina* **2022**, *42*, 2176–2183. [CrossRef] [PubMed]
47. Khandhadia, S.; Trump, D.; Menon, G.; Lotery, A.J. X-linked retinoschisis maculopathy treated with topical dorzolamide, and relationship to genotype. *Eye* **2011**, *25*, 922–928. [CrossRef] [PubMed]
48. Bucher, K.; Rodriguez-Bocanegra, E.; Dauletbekov, D.; Fischer, M.D. Immune responses to retinal gene therapy using adeno-associated viral vectors—Implications for treatment success and safety. *Prog. Retin. Eye Res.* **2021**, *83*, 100915. [CrossRef] [PubMed]
49. Cukras, C.; Wiley, H.E.; Jeffrey, B.G.; Sen, H.N.; Turriff, A.; Zeng, Y.; Vijayasathy, C.; Marangoni, D.; Ziccardi, L.; Kjellstrom, S.; et al. Retinal AAV8-RS1 Gene Therapy for X-Linked Retinoschisis: Initial Findings from a Phase I/IIa Trial by Intravitreal Delivery. *Mol. Ther.* **2018**, *26*, 2282–2294. [CrossRef] [PubMed]
50. Cheng, S.Y.; Punzo, C. Update on Viral Gene Therapy Clinical Trials for Retinal Diseases. *Hum. Gene Ther.* **2022**, *33*, 865–878. [CrossRef] [PubMed]
51. Hutton, D. Atsena Therapeutics Receives FDA Clearance of IND Application for ATSN-201 Investigational Gene Therapy for Treatment of X-Linked Retinoschisis. Available online: <https://atsenatx.com/press-release/atsena-therapeutics-receives-fda-clearance-of-ind-application-for-atsn-201-an-investigational-gene-therapy-for-the-treatment-of-x-linked-retinoschisis/> (accessed on 1 May 2023).
52. Furukawa, T.; Morrow, E.M.; Cepko, C.L. Crx, a novel otx-like homeobox gene, shows photoreceptor-specific expression and regulates photoreceptor differentiation. *Cell* **1997**, *91*, 531–541. [CrossRef]
53. Freund, C.L.; Gregory-Evans, C.Y.; Furukawa, T.; Papaioannou, M.; Looser, J.; Ploder, L.; Bellingham, J.; Ng, D.; Herbrick, J.A.; Duncan, A.; et al. Cone-rod dystrophy due to mutations in a novel photoreceptor-specific homeobox gene (CRX) essential for maintenance of the photoreceptor. *Cell* **1997**, *91*, 543–553. [CrossRef]
54. Lines, M.A.; Hébert, M.; McTaggart, K.E.; Flynn, S.J.; Tennant, M.T.; MacDonald, I.M. Electrophysiologic and phenotypic features of an autosomal cone-rod dystrophy caused by a novel CRX mutation. *Ophthalmology* **2002**, *109*, 1862–1870. [CrossRef]
55. Molday, R.S.; Hicks, D.; Molday, L. Peripherin. A rim-specific membrane protein of rod outer segment discs. *Investig. Ophthalmol. Vis. Sci.* **1987**, *28*, 50–61.
56. Arikawa, K.; Molday, L.L.; Molday, R.S.; Williams, D.S. Localization of peripherin/rds in the disk membranes of cone and rod photoreceptors: Relationship to disk membrane morphogenesis and retinal degeneration. *J. Cell Biol.* **1992**, *116*, 659–667. [CrossRef] [PubMed]



57. Nishiguchi, K.M.; Kunikata, H.; Fujita, K.; Hashimoto, K.; Koyanagi, Y.; Akiyama, M.; Ikeda, Y.; Momozawa, Y.; Sonoda, K.H.; Murakami, A.; et al. Association of CRX genotypes and retinal phenotypes confounded by variable expressivity and electronegative electroretinogram. *Clin. Exp. Ophthalmol.* **2020**, *48*, 644–657. [[CrossRef](#)] [[PubMed](#)]
58. Chapi, M.; Sabbaghi, H.; Suri, F.; Alehabib, E.; Rahimi-Aliabadi, S.; Jamali, F.; Jamshidi, J.; Emamalizadeh, B.; Darvish, H.; Mirrahimi, M.; et al. Incomplete penetrance of CRX gene for autosomal dominant form of cone-rod dystrophy. *Ophthalmic Genet.* **2019**, *40*, 259–266. [[CrossRef](#)] [[PubMed](#)]
59. Wang, Q.L.; Chen, S.; Esumi, N.; Swain, P.K.; Haines, H.S.; Peng, G.; Melia, B.M.; McIntosh, I.; Heckenlively, J.R.; Jacobson, S.G.; et al. QRX, a novel homeobox gene, modulates photoreceptor gene expression. *Hum. Mol. Genet.* **2004**, *13*, 1025–1040. [[CrossRef](#)] [[PubMed](#)]
60. Gregory-Evans, K.; Kelsell, R.E.; Gregory-Evans, C.Y.; Downes, S.M.; Fitzke, F.W.; Holder, G.E.; Simunovic, M.; Mollon, J.D.; Taylor, R.; Hunt, D.M.; et al. Autosomal dominant cone-rod retinal dystrophy (CORD6) from heterozygous mutation of GUCY2D, which encodes retinal guanylate cyclase. *Ophthalmology* **2000**, *107*, 55–61. [[CrossRef](#)] [[PubMed](#)]
61. Boon, C.J.; den Hollander, A.I.; Hoyng, C.B.; Cremers, F.P.; Klevering, B.J.; Keunen, J.E. The spectrum of retinal dystrophies caused by mutations in the peripherin/RDS gene. *Prog. Retin. Eye Res.* **2008**, *27*, 213–235. [[CrossRef](#)] [[PubMed](#)]
62. Ba-Abbad, R.; Robson, A.G.; Yap, Y.C.; Moore, A.T.; Webster, A.R.; Holder, G.E. Prph2 mutations as a cause of electronegative ERG. *Retina* **2014**, *34*, 1235–1243. [[CrossRef](#)]
63. Yamamoto, H.; Simon, A.; Eriksson, U.; Harris, E.; Berson, E.L.; Dryja, T.P. Mutations in the gene encoding 11-cis retinal dehydrogenase cause delayed dark adaptation and fundus albipunctatus. *Nat. Genet.* **1999**, *22*, 188–191. [[CrossRef](#)]
64. Schmitz-Valckenberg, S.; Pfau, M.; Fleckenstein, M.; Staurengi, G.; Sparrow, J.R.; Bindewald-Wittich, A.; Spaide, R.F.; Wolf, S.; Sadda, S.R.; Holz, F.G. Fundus autofluorescence imaging. *Prog. Retin. Eye Res.* **2021**, *81*, 100893. [[CrossRef](#)]
65. Sergouniotis, P.I.; Sohn, E.H.; Li, Z.; McBain, V.A.; Wright, G.A.; Moore, A.T.; Robson, A.G.; Holder, G.E.; Webster, A.R. Phenotypic variability in RDH5 retinopathy (Fundus Albipunctatus). *Ophthalmology* **2011**, *118*, 1661–1670. [[CrossRef](#)]
66. Wang, N.K.; Chuang, L.H.; Lai, C.C.; Chou, C.L.; Chu, H.Y.; Yeung, L.; Chen, Y.P.; Chen, K.J.; Wu, W.C.; Chen, T.L.; et al. Multimodal fundus imaging in fundus albipunctatus with RDH5 mutation: A newly identified compound heterozygous mutation and review of the literature. *Doc. Ophthalmol.* **2012**, *125*, 51–62. [[CrossRef](#)] [[PubMed](#)]
67. Nakamura, M.; Skalet, J.; Miyake, Y. RDH5 gene mutations and electroretinogram in fundus albipunctatus with or without macular dystrophy: RDH5 mutations and ERG in fundus albipunctatus. *Doc. Ophthalmol.* **2003**, *107*, 3–11. [[CrossRef](#)] [[PubMed](#)]
68. Krill, A.E.; Folk, M.R. Retinitis punctata albescens. A functional evaluation of an unusual case. *Am. J. Ophthalmol.* **1962**, *53*, 450–455. [[CrossRef](#)] [[PubMed](#)]
69. Fishman, G.A.; Roberts, M.F.; Derlacki, D.J.; Grimsby, J.L.; Yamamoto, H.; Sharon, D.; Nishiguchi, K.M.; Dryja, T.P. Novel mutations in the cellular retinaldehyde-binding protein gene (RLBP1) associated with retinitis punctata albescens: Evidence of interfamilial genetic heterogeneity and fundus changes in heterozygotes. *Arch. Ophthalmol.* **2004**, *122*, 70–75. [[CrossRef](#)] [[PubMed](#)]
70. Chen, J.; Rattner, A.; Nathans, J. The rod photoreceptor-specific nuclear receptor Nr2e3 represses transcription of multiple cone-specific genes. *J. Neurosci.* **2005**, *25*, 118–129. [[CrossRef](#)] [[PubMed](#)]
71. Audo, I.; Michaelides, M.; Robson, A.G.; Hawlina, M.; Vaclavik, V.; Sandbach, J.M.; Neveu, M.M.; Hogg, C.R.; Hunt, D.M.; Moore, A.T.; et al. Phenotypic variation in enhanced S-cone syndrome. *Investig. Ophthalmol. Vis. Sci.* **2008**, *49*, 2082–2093. [[CrossRef](#)] [[PubMed](#)]
72. Sharon, D.; Sandberg, M.A.; Caruso, R.C.; Berson, E.L.; Dryja, T.P. Shared mutations in NR2E3 in enhanced S-cone syndrome, Goldmann-Favre syndrome, and many cases of clumped pigmentary retinal degeneration. *Arch. Ophthalmol.* **2003**, *121*, 1316–1323. [[CrossRef](#)]
73. Khan, A.O.; Aldahmesh, M.; Meyer, B. The enhanced S-cone syndrome in children. *BMJ Case Rep.* **2009**, *2009*, bcr1020081163. [[CrossRef](#)]
74. Hull, S.; Arno, G.; Sergouniotis, P.I.; Tiffin, P.; Borman, A.D.; Chandra, A.; Robson, A.G.; Holder, G.E.; Webster, A.R.; Moore, A.T. Clinical and molecular characterization of enhanced S-cone syndrome in children. *JAMA Ophthalmol.* **2014**, *132*, 1341–1349. [[CrossRef](#)]
75. Zerbib, J.; Blanco Garavito, R.; Gerber, S.; Oubraham, H.; Sikorav, A.; Audo, I.; Kaplan, J.; Rozet, J.M.; Souied, E.H. Retinochoroidal anastomosis associated with enhanced s-cone syndrome. *Retin. Cases Brief Rep.* **2019**, *13*, 295–299. [[CrossRef](#)]
76. Yzer, S.; Barbazetto, I.; Allikmets, R.; van Schooneveld, M.J.; Bergen, A.; Tsang, S.H.; Jacobson, S.G.; Yannuzzi, L.A. Expanded clinical spectrum of enhanced S-cone syndrome. *JAMA Ophthalmol.* **2013**, *131*, 1324–1330. [[CrossRef](#)] [[PubMed](#)]
77. Wang, N.K.; Fine, H.F.; Chang, S.; Chou, C.L.; Cella, W.; Tosi, J.; Lin, C.S.; Nagasaki, T.; Tsang, S.H. Cellular origin of fundus autofluorescence in patients and mice with a defective NR2E3 gene. *Br. J. Ophthalmol.* **2009**, *93*, 1234–1240. [[CrossRef](#)] [[PubMed](#)]
78. Wang, N.K.; Lai, C.C.; Liu, C.H.; Yeh, L.K.; Chou, C.L.; Kong, J.; Nagasaki, T.; Tsang, S.H.; Chien, C.L. Origin of fundus hyperautofluorescent spots and their role in retinal degeneration in a mouse model of Goldmann-Favre syndrome. *Dis. Model Mech.* **2013**, *6*, 1113–1122. [[CrossRef](#)] [[PubMed](#)]
79. Liu, W.; Liu, S.; Li, P.; Yao, K. Retinitis Pigmentosa: Progress in Molecular Pathology and Biotherapeutical Strategies. *Int. J. Mol. Sci.* **2022**, *23*, 4883. [[CrossRef](#)] [[PubMed](#)]
80. Takahashi, V.K.L.; Takiuti, J.T.; Jauregui, R.; Mahajan, V.B.; Tsang, S.H. Rates of Bone Spicule Pigment Appearance in Patients With Retinitis Pigmentosa Sine Pigmento. *Am. J. Ophthalmol.* **2018**, *195*, 176–180. [[CrossRef](#)] [[PubMed](#)]
81. Wu, H.; Cowing, J.A.; Michaelides, M.; Wilkie, S.E.; Jeffery, G.; Jenkins, S.A.; Mester, V.; Bird, A.C.; Robson, A.G.; Holder, G.E.; et al. Mutations in the gene KCNV2 encoding a voltage-gated potassium channel subunit cause “cone dystrophy with supernormal rod electroretinogram” in humans. *Am. J. Hum. Genet.* **2006**, *79*, 574–579. [[CrossRef](#)] [[PubMed](#)]

82. Lenis, T.L.; Dhrami-Gavazi, E.; Lee, W.; Mukkamala, S.K.; Tabacaru, M.R.; Yannuzzi, L.; Gouras, P.; Tsang, S.H. Novel Compound Heterozygous Mutations Resulting in Cone Dystrophy With Supernormal Rod Response. *JAMA Ophthalmol.* **2013**, *131*, 1482–1485. [[CrossRef](#)]
83. Abdelkader, E.; Yasir, Z.H.; Khan, A.M.; Raddadi, O.; Khandekar, R.; Alateeq, N.; Nowilaty, S.; AlShahrani, N.; Schatz, P. Analysis of retinal structure and function in cone dystrophy with supernormal rod response. *Doc. Ophthalmol.* **2020**, *141*, 23–32. [[CrossRef](#)]
84. Liu, P.K.; Ryu, J.; Yeh, L.K.; Chen, K.J.; Tsang, S.H.; Liu, L.; Wang, N.K. A novel KCNV2 mutation in a patient taking hydroxychloroquine associated with cone dystrophy with supernormal rod response. *Ophthalmic Genet.* **2021**, *42*, 458–463. [[CrossRef](#)]
85. Ding, H.J.; Denniston, A.K.; Rao, V.K.; Gordon, C. Hydroxychloroquine-related retinal toxicity. *Rheumatology* **2015**, *55*, 957–967. [[CrossRef](#)]
86. Chen, E.; Brown, D.M.; Benz, M.S.; Fish, R.H.; Wong, T.P.; Kim, R.Y.; Major, J.C. Spectral domain optical coherence tomography as an effective screening test for hydroxychloroquine retinopathy (the “flying saucer” sign). *Clin. Ophthalmol.* **2010**, *4*, 1151–1158. [[CrossRef](#)] [[PubMed](#)]
87. Rosenbaum, J.T.; Costenbader, K.H.; Desmarais, J.; Ginzler, E.M.; Fett, N.; Goodman, S.M.; O’Dell, J.R.; Schmajuk, G.; Werth, V.P.; Melles, R.B.; et al. American College of Rheumatology, American Academy of Dermatology, Rheumatologic Dermatology Society, and American Academy of Ophthalmology 2020 Joint Statement on Hydroxychloroquine Use With Respect to Retinal Toxicity. *Arthritis Rheumatol.* **2021**, *73*, 908–911. [[CrossRef](#)] [[PubMed](#)]
88. Koh, V.; Tan, C.; Nah, G.; Zhao, P.; Yang, A.; Lin, S.T.; Wong, T.Y.; Saw, S.M.; Chia, A. Correlation of structural and electrophysiological changes in the retina of young high myopes. *Ophthalmic Physiol. Opt.* **2014**, *34*, 658–666. [[CrossRef](#)] [[PubMed](#)]
89. Sachidanandam, R.; Ravi, P.; Sen, P. Effect of axial length on full-field and multifocal electroretinograms. *Clin. Exp. Optom.* **2017**, *100*, 668–675. [[CrossRef](#)] [[PubMed](#)]
90. Gupta, S.K.; Chakraborty, R.; Verkicharla, P.K. Correction to: Electroretinogram responses in myopia: A review. *Doc. Ophthalmol.* **2022**, *145*, 97–98. [[CrossRef](#)] [[PubMed](#)]
91. Yin, R.; Xu, Z.; Mei, M.; Chen, Z.; Wang, K.; Liu, Y.; Tang, T.; Priyadarshi, M.K.; Meng, X.; Zhao, S.; et al. Soft transparent graphene contact lens electrodes for conformal full-cornea recording of electroretinogram. *Nat. Commun.* **2018**, *9*, 2334. [[CrossRef](#)] [[PubMed](#)]
92. Dockery, A.; Whelan, L.; Humphries, P.; Farrar, G.J. Next-Generation Sequencing Applications for Inherited Retinal Diseases. *Int. J. Mol. Sci.* **2021**, *22*, 5684. [[CrossRef](#)]
93. Fadaie, Z.; Khan, M.; Del Pozo-Valero, M.; Cornelis, S.S.; Ayuso, C.; Cremers, F.P.M.; Roosing, S.; The Abca Study, G. Identification of splice defects due to noncanonical splice site or deep-intronic variants in ABCA4. *Hum. Mutat.* **2019**, *40*, 2365–2376. [[CrossRef](#)]
94. Qian, X.; Wang, J.; Wang, M.; Igelman, A.D.; Jones, K.D.; Li, Y.; Wang, K.; Goetz, K.E.; Birch, D.G.; Yang, P.; et al. Identification of Deep-Intronic Splice Mutations in a Large Cohort of Patients With Inherited Retinal Diseases. *Front. Genet.* **2021**, *12*, 647400. [[CrossRef](#)]
95. Cornish, E.E.; Vaze, A.; Jamieson, R.V.; Grigg, J.R. The electroretinogram in the genomics era: Outer retinal disorders. *Eye* **2021**, *35*, 2406–2418. [[CrossRef](#)]
96. Richards, S.; Aziz, N.; Bale, S.; Bick, D.; Das, S.; Gastier-Foster, J.; Grody, W.W.; Hegde, M.; Lyon, E.; Spector, E.; et al. Standards and guidelines for the interpretation of sequence variants: A joint consensus recommendation of the American College of Medical Genetics and Genomics and the Association for Molecular Pathology. *Genet. Med.* **2015**, *17*, 405–424. [[CrossRef](#)] [[PubMed](#)]
97. Qiao, D.; Lange, C.; Laird, N.M.; Won, S.; Hersh, C.P.; Morrow, J.; Hobbs, B.D.; Lutz, S.M.; Ruczinski, I.; Beaty, T.H.; et al. Gene-based segregation method for identifying rare variants in family-based sequencing studies. *Genet. Epidemiol.* **2017**, *41*, 309–319. [[CrossRef](#)] [[PubMed](#)]
98. Jayanna, S.; Jalali, S.; Padhi, T.R.; Agarwal, K.; Chhablani, J. OCT Imaging in Infants. *Semin Ophthalmol.* **2022**, *37*, 358–372. [[CrossRef](#)] [[PubMed](#)]
99. Magnúsdóttir, V.; Vehmeijer, W.B.; Eliasdóttir, T.S.; Hardarson, S.H.; Schalijs-Delfos, N.E.; Stefánsson, E. Fundus imaging in newborn children with wide-field scanning laser ophthalmoscope. *Acta Ophthalmol.* **2017**, *95*, 842–844. [[CrossRef](#)] [[PubMed](#)]
100. Tremblay, F.; Parkinson, J.E.; Lalonde, M.R. Anesthesia and Electroretinography. *Investig. Ophthalmol. Vis. Sci.* **2003**, *44*, 1897.
101. Mahroo, O.A. Visual electrophysiology and “the potential of the potentials”. *Eye* **2023**, *37*, 2399–2408. [[CrossRef](#)] [[PubMed](#)]
102. Carter, P.; Gordon-Reid, A.; Shawkat, F.; Self, J.E. Comparison of the handheld RETeval ERG system with a routine ERG system in healthy adults and in paediatric patients. *Eye* **2021**, *35*, 2180–2189. [[CrossRef](#)] [[PubMed](#)]
103. You, J.Y.; Dorfman, A.L.; Gauvin, M.; Vatcher, D.; Polomeno, R.C.; Little, J.M.; Lachapelle, P. Comparing the RETeval® portable ERG device with more traditional tabletop ERG systems in normal subjects and selected retinopathies. *Doc. Ophthalmol.* **2023**, *146*, 137–150. [[CrossRef](#)]
104. Glington, S.L.; Calcagni, A.; Lilaonitkul, W.; Pontikos, N.; Vermeirsch, S.; Zhang, G.; Arno, G.; Wagner, S.K.; Michaelides, M.; Keane, P.A.; et al. Phenotyping of ABCA4 Retinopathy by Machine Learning Analysis of Full-Field Electroretinography. *Transl. Vis. Sci. Technol.* **2022**, *11*, 34. [[CrossRef](#)]
105. Gajendran, M.K.; Rohowetz, L.J.; Koulen, P.; Mehdizadeh, A. Novel Machine-Learning Based Framework Using Electroretinography Data for the Detection of Early-Stage Glaucoma. *Front. Neurosci.* **2022**, *16*, 869137. [[CrossRef](#)]
106. Schwitzer, T.; Leboyer, M.; Laprévotte, V.; Louis Dorr, V.; Schwan, R. Using retinal electrophysiology toward precision psychiatry. *Eur. Psychiatry* **2022**, *65*, e9. [[CrossRef](#)]

**Disclaimer/Publisher’s Note:** The statements, opinions and data contained in all publications are solely those of the individual author(s) and contributor(s) and not of MDPI and/or the editor(s). MDPI and/or the editor(s) disclaim responsibility for any injury to people or property resulting from any ideas, methods, instructions or products referred to in the content.